

Spring 2015

Measurement Of Multidirectional Thermal Properties Of As4/ 3501-6 Unidirectional Composite Laminate

Ali Adam Osman
North Carolina Agricultural and Technical State University

Follow this and additional works at: <https://digital.library.ncat.edu/theses>

Recommended Citation

Osman, Ali Adam, "Measurement Of Multidirectional Thermal Properties Of As4/3501-6 Unidirectional Composite Laminate" (2015). *Theses*. 270.
<https://digital.library.ncat.edu/theses/270>

This Thesis is brought to you for free and open access by the Electronic Theses and Dissertations at Aggie Digital Collections and Scholarship. It has been accepted for inclusion in Theses by an authorized administrator of Aggie Digital Collections and Scholarship. For more information, please contact iyanna@ncat.edu.

Measurement of Multidirectional Thermal Properties of AS4/3501-6 Unidirectional
Composite Laminate

Ali Adam Osman

North Carolina A&T State University

A thesis submitted to the graduate faculty
in partial fulfillment of the requirements for the degree of

MASTER OF SCIENCE

Department: Mechanical Engineering

Major: Mechanical Engineering

Major Professor: Dr. Kunigal Shivakumar

Greensboro, North Carolina

2015

The Graduate School
North Carolina Agricultural and Technical State University

This is to certify that the Master's Thesis of

Ali Adam Osman

has met the thesis requirements of
North Carolina Agricultural and Technical State University

Greensboro, North Carolina

2015

Approved by:

Dr. Kunigal Shivakumar
Major Professor

Dr. Dhananjay Kumar
Committee Member

Dr. Sandi Miller (NASA, GRC)
Committee Member

Dr. Samuel Owusu-Ofori
Department Chair

Dr. Sanjiv Sarin
Dean, The Graduate School

Biographical Sketch

Ali Adam Osman was born in AL-Azzazi, Sudan. He earned his Bachelor of Science degree in Mechanical Engineering from Sudan University of Science & Technology in 2005. His hometown is located in Khartoum. Ali's zeal for knowledge and great dedication to reach his goals were possible with his parents' continued support and encouragement. He is currently a candidate for the Masters of Science degree in Mechanical Engineering.

Dedication

I dedicate this Master's Thesis to my family and friends, for their love, and continuous support. I humbly, dedicate this work to my God, for his, protection and favor.

Acknowledgements

I would like to extend my sincerest appreciation to my advisor Dr. Kunigal Shivakumar for being an informative and supportive advisor during challenging times in the course of the research. I wish to express my acknowledgement to my thesis committee members, Dr. Dhananjay Kumar and Sandi Miller for their time to review and offer constructive criticism of my thesis. Also I would like to thank Dr. Messiha Saad for introducing me to the field of thermal science. I express my sincere thanks to the department of mechanical engineering and Samuel Owusu-Ofori providing financial support during my education.

I would like thank the staff and faculty of Center of Composite Material Research (CCMR), Center of Aviation Safety (CAS) and Department of Mechanical Engineering for their support during my studies and research. Especial thanks to Mr. Mathew Sharpe, Composite Material Lab Manager for his help in fabricating composite laminates, preparation of test specimens and testing. I also would like to acknowledge the support of the other staff, Dr. Raghu Panduranga and Mr. John Skujins for their encouragement and guidance. I must also thank former and current students of CCMR: Hiba Ahmed, Kazi Imran, Furkan Ulu, Torrance Marunda, Sidharth Karnati and Russell Smyre.

Table of Contents

List of Figures	x
List of Tables	xii
Abstract	1
1. CHAPTER 1 Introduction.....	2
1.1 Background.....	2
1.2 Thermal Properties of Composite Materials	5
1.3 Literature Review on Thermal Properties of Composite Materials	5
1.3.1 Experimental approach.....	6
1.3.1.1 Thermographic method	6
1.3.1.2 Thermal Wave Interferometry (TWI) method.....	7
1.3.2 Thermal conductivity based on micromechanics.	9
1.4 AS4/3501-6 Carbon/Epoxy Composites Material	11
1.5 The Objectives of the Research	12
1.6 Scope of This Thesis.....	12
2. CHAPTER 2 Experimental Approach	14
2.1 Introduction.....	14
2.2 An Approach of Measuring Thermal Conductivity (k)	14
2.3 Measurement of Specific Heat Capacity (C_p).....	15
2.4 Measurement of Thermal Diffusivity (α)	19
2.5 Validation of Methodology.....	22
2.6 Laminate and Specimens Preparation for Unidirectional Composites	23
2.7 Summary.....	24

3. CHAPTER 3 AS4/3501-6 Carbon/Epoxy Composite Material Samples Preparation.....	26
3.1 Introduction.....	26
3.2 Fabrication of Panels	26
3.3 Preparation Specimen for Diffusivity Test.	27
3.4 Specimens Preparation for Diffusivity Measurement.....	28
3.5 Specimen Preparation for Specific Heat Test	31
3.6 Optical Microscopy of the Specimen	32
3.7 Special Test Studies.....	34
3.8 Summary.....	34
4. CHAPTER 4 Experiments and Results.....	35
4.1 Introduction.....	35
4.2 Measurement of Specific Heat Capacity (C_p).....	35
4.2.1 Test preparation.	35
4.2.2 Test procedure and data.....	36
4.3 Measurement of the Thermal Diffusivity (α)	40
4.3.1 Software setup	41
4.3.2 Testing.....	41
4.3.4 Transverse thermal diffusivity (α_3).....	46
4.3.5 Summary.....	49
4.4 Calculation of Thermal Conductivity (k).....	49
4.5 Special Assessment.....	52
4.5.1 The thickness affects.	52
4.5.2 Surface coating of specimen.....	56
4.6 Summary.....	58

5. CHAPTER 5 Thermal Conductivity Prediction by Micromechanics	60
5.1 Introduction.....	60
5.2 Unit Cell Model	60
5.3 Axial Thermal Conductivity (k_1)	61
5.4 Transverse Conductivity (k_3)	62
5.5 Models and Comparison	62
5.6 Prediction of the Transverse Conductivity (k_3) for AS4/3501-6 Composite	65
5.7 Summary.....	65
6. CHAPTER 6 Concluding Remarks and Future Work	67
6.1 Concluding Remarks	67
6.2 Future Work.....	68
7. References.....	69

List of Figures

Figure 1.1 Classification of Composite material system [1].....	4
Figure 1.2 Experimental set up of the Thermographic method	7
Figure 1.3 Thermal Wave Interferometry experimental set up.....	8
Figure 2.1 Netzsch Differential Scanning Calorimeter.....	16
Figure 2.2 Netzsch DSC Cross Section View.....	17
Figure 2.3 Flashline 2000 Thermal Properties Analyzer	19
Figure 2.4 Schematic of the Flash Method	21
Figure 2.5 Principal directions of unidirectional composites and specimens extraction for transverse diffusivity measurement	24
Figure 2.6 Principal directions of unidirectional composites and specimens extraction for axial diffusivity measurement.....	24
Figure 3.1 AS4/3501-6 composite prepreg for laminates fabrication.....	27
Figure 3.2 The principal directions of laminated composite material	28
Figure 3.3 Drilling machine used to cut AS4/3501-6 composite laminate.....	29
Figure 3.4 Axial specimen geometry and photograph	29
Figure 3.5 Model and photograph of through the thickness diffusivity measurement.	30
Figure 3.6 Specimens prepared for specific heat capacity test	31
Figure 3.7 Nikon eclipse LV150 microscope.....	32
Figure 3.8 Thin specimen (through –the – thickness) measurement model and optical image of the specimen on $x_1 - x_2$ plane.....	33
Figure 3.9 Thick specimen (axial measurement) model and optical images of $x_2 - x_3$ plane at 10, 20 and 50 magnifications.....	33

Figure 4.1 Top view of specimen placed on the heat flux Sensor [20]	36
Figure 4.2 Specific heat capacity plot of tested specimens	37
Figure 4.3 Average specific heat capacity and its error	39
Figure 4.4 Block diagram of the Flash line 2000 Thermal Properties Analyzer	40
Figure 4.5 Photo graph of top view of Flash line 2000 Thermal Properties Analyzer	41
Figure 4.6 The average axial thermal diffusivity (α_1).....	44
Figure 4.7 The average axial diffusivity with its standard deviation.....	45
Figure 4.8 The average transverse thermal diffusivity	48
Figure 4.9 The Transverse diffusivity with its standard deviation	49
Figure 4.10 The Average axial thermal conductivity	51
Figure 4.11 The average transverse thermal conductivity	52
Figure 4.12 The average axial thermal conductivity for 2mm thickness.....	55
Figure 4.13 Comparison between the axial thermal conductivities for different thicknesses	56
Figure 4.14 The axial thermal conductivity before and after coating.....	57
Figure 5.1 Description of the unit cell.	60

List of Tables

Table 1.1 Axial and transverse thermal conductivities of different types of composites.....	8
Table 1.2 Laminate mechanical properties of AS4/3501-6 carbon/epoxy composite [5].	12
Table 2.1 Typical data of DSC [11].....	15
Table 2.2 Technical Specifications of the DSC 200 F3 Maia®	16
Table 2.3 Technical Specifications of the Flash Line TM 2000 Thermal Properties Analyzer ...	20
Table 2.4 Typical data of thermal diffusivity of thermographite [14].....	20
Table 2.5 Thermal properties of carbon- carbon composite at room temperature [17].....	22
Table 3.1 Fabricated AS4/3501-6 carbon/Epoxy material properties [18].....	27
Table 3.2 Specimen for axial diffusivity (α_1) measurement.	30
Table 3.3 Specimen for transverse diffusivity (α_3) measurement.....	30
Table 3.4 Physical Properties of Specimens for specific heat capacity test	31
Table 4.1 Specific heat capacity (Cp) results of AS4/3501-6 carbon/Epoxy	37
Table 4.2 Specific heat capacity results of AS4/3501-6 carbon/Epoxy.....	39
Table 4.3 Axial thermal diffusivity (α_1) of Sp #1 and Sp #2.....	43
Table 4.4 Axial thermal diffusivity (α_1) of Sp #3 and Sp #4	43
Table 4.5 Axial thermal diffusivity (α_1) of Sp #5	44
Table 4.6 Percentage error of the thermal the axial diffusivity (α_1)	45
Table 4.7 Transverse thermal diffusivity data of Sp #1 and Sp #2.....	46
Table 4.8 Transverse thermal diffusivity data of Sp #3 and Sp #4.....	47
Table 4.9 Transverse thermal diffusivity data of Sp #5.....	47
Table 4.10 The results for the transverse thermal diffusivity and standard deviation	48
Table 4.11 Calculated axial thermal conductivity (k_1) of specimens	50

Table 4.12 Calculated transverse thermal conductivity (k_3) of specimens.....	51
Table 4.13 Axial thermal diffusivity (α_1) of Sp #1 and Sp #2.....	53
Table 4.14 Axial thermal diffusivity (α_1) of Sp #3 and Sp #4.....	54
Table 4.15 Axial thermal diffusivity (α_1) of Sp #5.....	54
Table 4.16 Axial thermal conductivity data for 2mm thickness.....	55
Table 4.17 Comparison of the axial thermal conductivity before and after coating.....	57
Table 5.1 Constituent properties of AS4 graphite/ epoxy and AS4/3501-6 composite material..	61
Table 5.2 Comparison between models.....	65
Table 5.3 Comparison between predicted transverse conductivity (k_3) and experimental results	65

Abstract

Thermal characterization of composite materials is important in the design of thermal systems, including applications such as aerospace, automotive, etc. These material properties are lacking in the literature and they need to be established considering the multidirectional behavior of the composite materials. Knowing multidirectional thermal properties of AS4/3501-6 composite laminate are essential in the engineering design and control process. By selecting the appropriate combination of matrix and reinforcement of material, designers have the ability to design and construct a material with specified properties. This research focuses on thermal conductivity characterization of AS4/3501-6 unidirectional composite material. The objective of this research is to determine axial and transverse thermal conductivity of AS4/3501-6 carbon/epoxy composite laminate by experiment and micromechanics models in literature. AS4/3501-6 unidirectional composite laminate was fabricated using autoclave process; two laminates were made, thick for axial and thin for transverse property testing. Flash method was used to measure the thermal diffusivity in axial and transverse directions of the fiber according to the ASTM E-1461 standard. Differential scanning calorimeter was used to measure the specific heat capacity of the laminate following ASTM E-1269 standard. Then the thermal conductivity was calculated by the product of specific heat, diffusivity and the material density. The properties were established at temperature range 20 °C to 100 °C. Test results were compared with micromechanics models and the literature data. The axial (k_1) and transverse (k_3) thermal conductivities at room temperature were 4.9 W/mK and 0.69 W/mK, respectively.

CHAPTER 1

Introduction

Thermal properties of composite materials such as thermal conductivity, specific heat capacity and thermal expansion play important roles in the design process and performance of composite structures. Studying the thermal properties of composites is an important part, especially for structures exposed to high temperature such as aerospace and power generation. Thermal conductivity determines the working temperature levels of composite materials when considering the performance in high temperature applications as well as safety, process control, and quality assurance. This chapter presents a background of unidirectional composite materials, thermal properties, advantage and disadvantage of composite materials. Literature review on experimental approaches and brief overviews of prediction models based on micromechanical models described. Finally, the material of interest, objectives of the research and the scope of the thesis are presented.

1.1 Background

A composite material is a structural material consists of two or more materials that are combined on microscopic level to form new and more valuable materials. The matrix materials support the reinforcement materials by maintaining the relative positions. The reinforcement provides the composite excellent thermal properties, mechanical strength and stiffness. One constituent is called the reinforcing phase and the second in which it is embedded is called the matrix. The reinforcing phase material may be in the form of fibers, particles, or flakes. The matrix phase materials are generally continuous. Examples of composite systems include concrete reinforced with steel and epoxy reinforced with graphite fibers, etc. Fiber reinforced composites are classified by the geometry of the reinforcement, or by the type of

matrix. Based on the geometry of reinforcement, composite materials are divided into two main categories; discontinuous and continuous fiber-reinforced composites as shown in Figure 1.1. Discontinuous-fiber composites include short fibers, flakes, fabric particles, and nanotubes. Continuous fiber reinforced composite materials recognized by the fact the fibers are long enough to participate in full load carrying. The fibers on this type could be unidirectional and/or multidirectional. Commercial reinforcements are available in different forms, such as plain weave, harness satins, braided, stitched and unidirectional tapes.

In addition, composite materials are also classified based on the type of matrix. They are classified as polymer matrix composites (PMC), metal matrix composites (MMC), and ceramic matrix composites (CMC). Polymer matrix composites consist of thermoset (polyamide, epoxy, polyester) or thermoplastic (poly-ether-ether-ketone, polysulfone) resins. These types of polymers reinforced with either carbon, graphite, glass, aramid (Kevlar), or boron fiber. Metal matrix composites includes metals or alloys such as copper, magnesium, aluminum, or titanium, reinforced with boron, carbon (graphite), or ceramic fibers. These types of composites are limited by the softening or melting temperature of the metal matrix. Ceramic matrix composites includes ceramic matrices such as aluminum oxide, silicon carbide, glass ceramic, and silicon nitride reinforced with ceramic fibers. These types of composites are suitable for high temperature applications [1]. Carbon-Carbon composites, includes carbon or graphite matrix reinforced with carbon fibers, these composites are a special class of ceramic matrix composites, which recognized with high resistance to thermal shock, high strength and stiffness at very high temperatures.

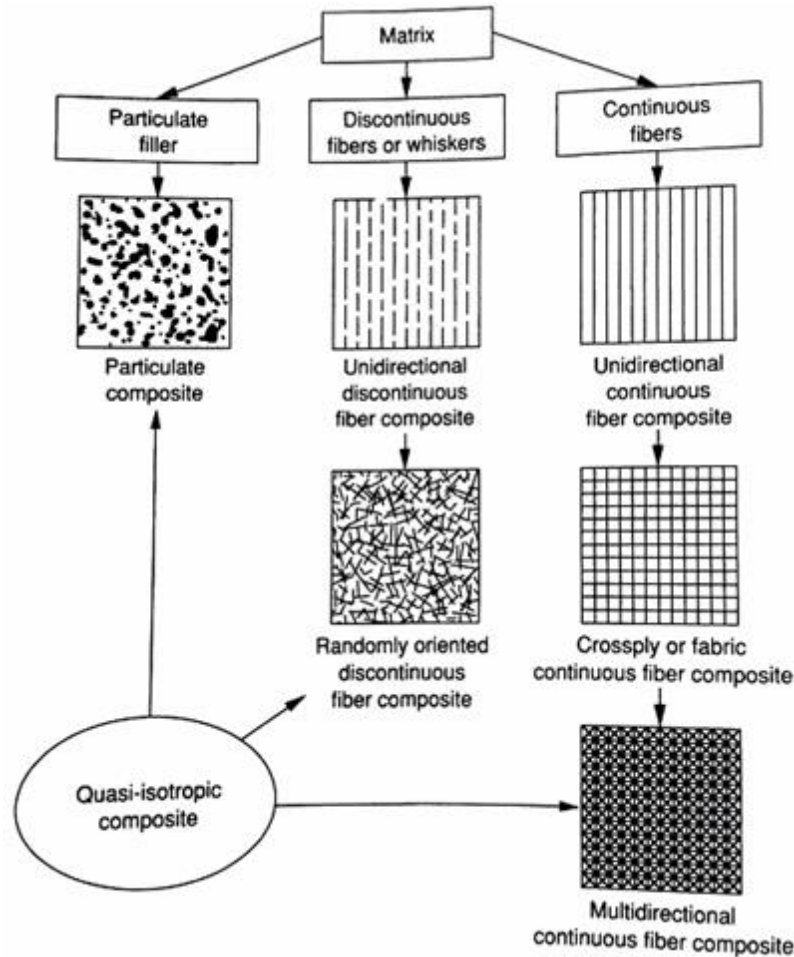


Figure 1.1 Classification of Composite material system [1]

Composites have several advantages over the metallic materials used nowadays. These advantages include high stiffness, high strength, lower density, longer fatigue life, corrosion resistance. Additionally, there are benefits such as increased wear resistance and improved thermal insulation. A structure of laminated composite performance relies on its high specific stiffness and high specific strength of the material. Its high specific stiffness stems from the materials modulus-to-density ratio, and the high specific strength stems from the materials strength-to-density ratio. By selecting the appropriate combination of matrix and reinforcement of material, designers have the ability to design and construct a material with specified properties.

On the other hand, there are disadvantages and limitations to composite materials. The most common problem of the composite laminate is the delamination. That occurs when the interlaminar stresses due to the dissimilarity between the anisotropic mechanical and thermal properties of the plies occurring at the free edges, joints and under out-of-plane loading. Delamination is the dominating failure mode in composite laminates.

1.2 Thermal Properties of Composite Materials

Composite materials are considered to be more important in the construction of aerospace structures. During the last ten years aircraft parts made from composite materials were developed for their weight savings over aluminum parts. New generation aircraft are designed with all composite material. The design and repair of these advanced composite structures requires an in-depth knowledge of mechanical as well as thermal properties. Composite structures are known to be highly anisotropic with low thermal conductivities. A structure made of reinforced composite material is generally a laminate made of various layers stacked on each other. Knowing the thermo-mechanical properties of a lamina is important to determine the laminate mechanical and thermal properties [1]. The literature lacks thermal conductivity properties of composite materials. Therefore, the focus of this research is measuring of thermal conductivities of fiber reinforced composites.

1.3 Literature Review on Thermal Properties of Composite Materials

There are some factors affect thermal properties of composite materials such as the moisture, density of material, and the ambient temperature. For example by increasing density, moisture and temperature the thermal conductivity increases. The thermal conductivity of composite material is always determined by two different approaches which are often applied for estimating thermal properties of composite materials. The first approach is based on heat

transfer measurements (experimental approaches), and the other one is based on micromechanics models

1.3.1 Experimental approach. This approach discloses measuring thermal diffusivity of composites based on heat transfer measurement in axial or transverse direction of the fiber, and then the thermal conductivity can be calculated by the product of the material density, specific heat and the diffusivity. Currently, methods used to measure thermal diffusivity of composite materials include Thermographic method [2], and Thermal wave Interferometry (TWI) method [3], and the most common used technique is Anter Flashline properties analyzer. In this research Anter Flashline and Differential Scanning Calorimeter (DSC) used to determine the thermal conductivity of AS4/3501-6 Carbon/Epoxy of the composite (prediction models).

1.3.1.1 Thermographic method. The Thermographic method is based on the heat transfer on the surface of an infinite slab that has been instantaneously heated by a Gaussian shaped source. This Technique is used to determine the thermal diffusivity of large diameter composites material specimen [2]. The sample usually heat treated at 1800 °C, 2100 °C and 2400°C, and then the thermal diffusivity measured. It found that the heat treated sample displayed higher thermal conductivity than non-treated sample because the crystallinity of the heat-treated sample when compared to the non-heat treated. Generally, thermal conductivity of composites increased with heat treatment temperature. Figure1.2 displays measurement of thermal diffusivity using Thermographic method.

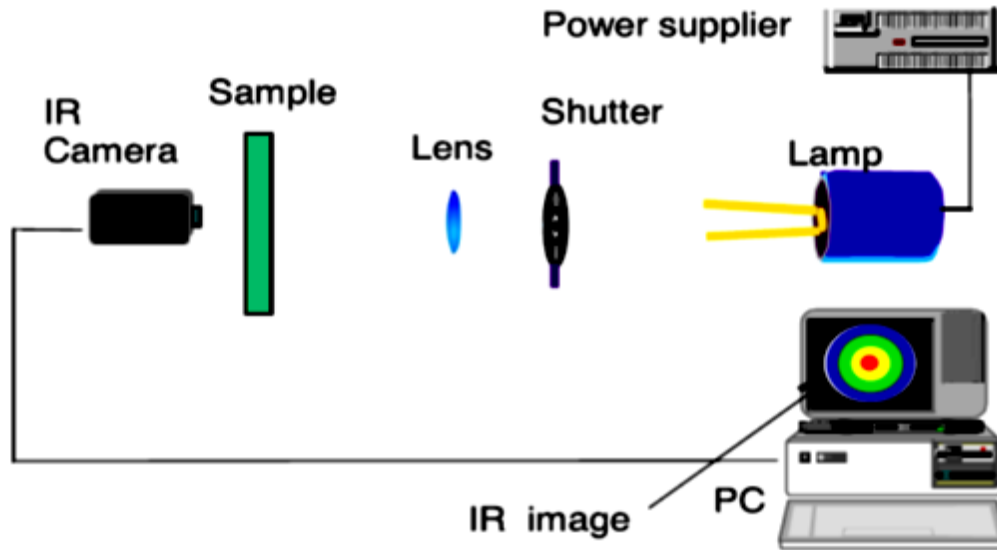


Figure 1.2 Experimental set up of the Thermographic method

1.3.1.2 Thermal Wave Interferometry (TWI) method. Thermal wave interferometry (TWI) technique is used to measure the diffusivity of thin slabs [3]. In this method the measurements conducted is based on the fact that thermal waves with angular frequencies will propagate through the material layers. The waves are reflected and then transmitted at the separation surface of the two different materials. The interference between reflected and propagating waves alters the phase and the amplitude of the AC component of the surface temperature. This method considered very complicated due to of multiple waves involvement. Figure 1.3 displays schematic of Thermal wave interferometry.

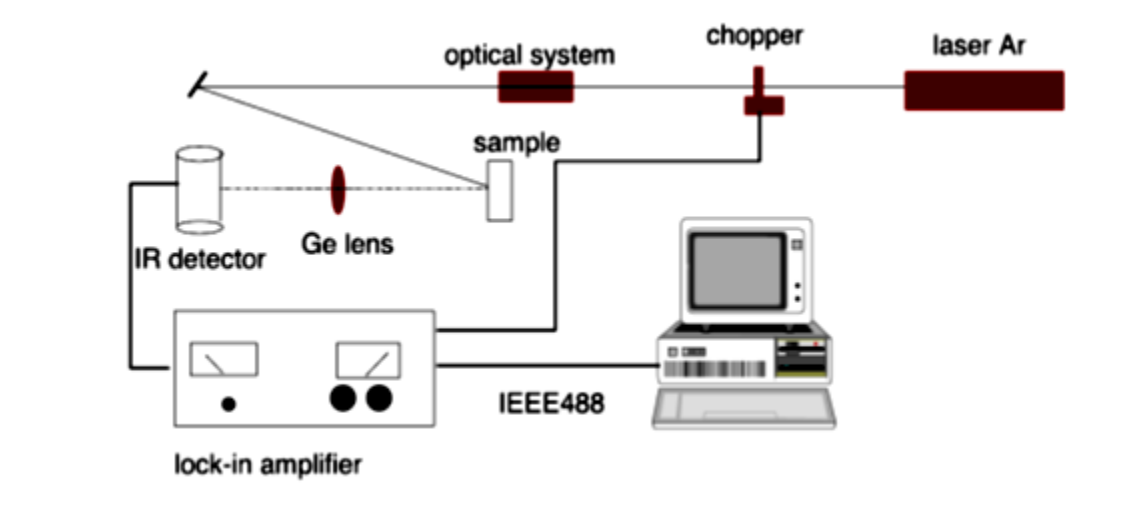


Figure 1.3 Thermal Wave Interferometry experimental set up.

Many researches [4-9] have measured axial and transverse thermal conductivities of composite materials. The results differ with each other depending on the matrix and fiber of the composite. The results of axial and transverse thermal conductivities of these researches listed in Table 1.1. Axial thermal conductivity value varies from 2 W/m k to 8 W/mK, higher than the transvers conductivity (0.3 W/mK to 0.8 W/mK).

Table 1.1

Axial and transverse thermal conductivities of different types of composites.

Material	Thermal Conductivity, k , W/mK	
	Axial, k_1	Transverse, k_3
Graphite/Epoxy, plain weave Composite [4]	5.36	0.43 - 0.5
AS4/3501-6 Carbon/Epoxy [5]	6.83	-
F593 Carbon/Epoxy [6]	2 - 3.5	0.5 - 0.8
Graphite/Epoxy Composite [7]	3.8-8.0	0.4 - 0.8
AS4/3501-6 Carbon/Epoxy [8]	-	0.61

1.3.2 Thermal conductivity based on micromechanics. This section explains calculating of thermal conductivity based on constituent components of the composite. The axial conductivity (k_1) was obtained by rule of mixtures (Equation 1.1)

$$k_1 = V_f k_{1f} + V_m k_m \quad (1.1)$$

where k_1, k_{1f} are the axial thermal conductivity of the composite and the fiber, respectively, V_f and V_m are the fiber and matrix volume fractions, and k_m is the matrix conductivity.

Below are six different models which have been reported in literature to predict the transverse thermal conductivity of unidirectional composites. These models assume the knowledge of the fiber and the matrix thermal properties (see Table 5.1), and fiber volume fraction of the composite.

1. Chawla model:

$$k_3 = k_m \left(\left(1 - \sqrt{V_f} \right) + \frac{\sqrt{V_f}}{1 - \sqrt{V_f} \left(1 - \frac{k_m}{k_{3f}} \right)} \right) \quad (1.2)$$

2. Springer-Tsai model:

$$k_3 = k_m \left[\left(1 - 2\sqrt{\frac{V_f}{\pi}} \right) + \frac{1}{B} \left[\pi - \frac{4}{\sqrt{1 - \left(\frac{B^2 V_f}{\pi} \right)}} \tan^{-1} \frac{\sqrt{1 - \left(\frac{B^2 V_f}{\pi} \right)}}{1 + B\sqrt{\frac{V_f}{\pi}}} \right] \right] \quad (1.3)$$

$$\text{where } B = 2 \left(\frac{K_m}{K_{3f}} - 1 \right)$$

3. Hashin model

$$k_3 = k_m + \frac{V_f}{\frac{1}{k_{3f} - k_m} + \frac{1 - V_f}{2km}} \quad (1.4)$$

4. Rayleigh model:

$$k_3 \approx k_m \left(1 - \frac{2V_f}{\nu' + V_f - \frac{C_1}{\nu'} V_f^4 - \frac{C_2}{\nu'} V_f^8} \right) \quad (1.5)$$

where $C_1 = 0.3058$, $C_2 = 0.0134$, and the expression for ν' is given by

$$\nu' = \frac{\frac{km}{k_{3f}} + 1}{\frac{k_m}{k_{3f}} - 1} \quad (1.6)$$

5. Farmer-Covert model K_3 same as Rayleigh except:

$$v' = \frac{\frac{k_m}{k_{3f}} + 1 + \frac{k_m}{ah_c}}{\frac{k_m}{k_{3f}} - 1 + \frac{k_m}{ah_c}} \quad (1.7)$$

here “a” is the fiber radius, and h_c is the interface conductance.

6. Halpin -Tsai model is given by:

$$k_3 = k_m \left[\frac{1 + \xi \eta V_f}{1 - \eta V_f} \right] \quad (1.8)$$

Where

$$\eta = \frac{\frac{k_{3f}}{k_m} - 1}{\frac{k_f}{k_m} + \xi} \quad (1.9)$$

when $\xi = 1$ Equation 1.7 can be written as:

$$k_3 = k_m \frac{V_f}{\frac{1}{k_f - k_m} + \frac{1 - V_f}{2k_m}} \quad (1.10)$$

1.4 AS4/3501-6 Carbon/Epoxy Composites Material

A prepreg of AS4/3501-6 carbon/epoxy composite material is supplied by the Hexcel Composites. The fiber areal weight was 150 g/m^2 with a resin content of 33%. The epoxy matrix is 3501-6 reinforced with unidirectional carbon fibers AS4. The laminate mechanical properties are listed in Table 1.2.

Table 1.2

Laminate mechanical properties of AS4/3501-6 carbon/epoxy composite [5].

Mechanical Properties	AS4/3501
0 ⁰ Tensile Strength, ksi	310
0 ⁰ Tensile Modulus, msi	20.5
0 ⁰ Compression Strength, ksi	250
0 ⁰ Flexural Strength, ksi	260
0 ⁰ Flexural Modulus, ksi	18.5
Short beam shear, ksi	9.5

1.5 The Objectives of the Research

The overall objective of this research is to determine thermal conductivity of AS4/3501-6 carbon/epoxy composite laminate in its principal material directions, and compare the results with literature data and current available micromechanics models

The Specific Objectives of the research are:

- (a) Determine thermal diffusivity using Flashline 2000 Thermal Properties Analyzer.
- (b) Determine specific heat capacity using Netzsch- Differential Scanning Calorimeter.
- (c) Calculate the thermal conductivities along and across the fiber directions of unidirectional composite laminate.
- (d) Compare the measured values with the micromechanics models and literature data.

1.6 Scope of This Thesis

This thesis has been organized into six chapters. Chapter1 has presented the background, present approach and literature review on thermal properties AS4/3501-6 carbon /epoxy composite laminates, as well as research objectives and the scope of the thesis. Chapter 2 describes experimental approach of thermal diffusivity and specific heat capacity measurement.

Chapter 3 describes AS4/3501-6 carbon /epoxy composite laminates laminate preparation, sample extraction, sample polishing and optical imaging. Chapter 4 provides an in-depth discussion of the testing and data analysis of specific heat capacity, thermal diffusivity and thermal conductivity. Chapter 5 explains prediction of thermal conductivity by micromechanics and comparison between several prediction models and with the literature data. Finally, chapter 6 presents conclusions and future work.

CHAPTER 2

Experimental Approach

2.1 Introduction

This chapter introduces experimental approach of specific heat capacity measurement using Netzsch Differential Scanning Calorimeter (DSC) device, and thermal diffusivity measurement using Anter Flashline 2000 Thermal Properties Analyzer. Validation of the test results using this method with the literature has reviewed. The specimen's preparation for measuring axial and transverse diffusivity of unidirectional composite material is also presented.

2.2 An Approach of Measuring Thermal Conductivity (k)

Thermal conductivity is defined as ability of material to conduct heat. It is measured in Watts per square meter of surface area for a temperature gradient of one Kelvin degree for one meter thickness of the material [9]. When the density, thermal diffusivity and specific capacity of an isotropic material are known, the thermal conductivity is calculated using Equation:

$$k = \rho \cdot C_p \cdot \alpha \quad (2.1)$$

where k is the thermal conductivity, ρ is the density, C_p is the specific heat capacity and α is the thermal diffusivity of the material. Once ρ , C_p , and α are measured the conductivity (k) can be calculated.

Flash method and differential scanning calorimeter are used to measure thermal diffusivity (α) and specific heat capacity (C_p), respectively. Calculating thermal conductivity with Equation 2.1 is simple, reliable, and accurate compared to the other methods in the literature [2, 3]. Furthermore both the flash and differential scanning calorimeter methods are recognized

by the American Society for Testing and Materials Standards as the standard methods to measure thermal diffusivity and specific heat capacity of the material.

2.3 Measurement of Specific Heat Capacity (C_p)

Specific heat capacity is a physical quantity that is defined as how much heat per unit mass is required to raise the temperature of a material one degree Celsius. Many methods have been used to measure specific heat capacity however differential scanning calorimeter demonstrated as the best technique [10] used to determine the specific heat of a material. The approach of this technique is based upon heat flow measurement of unknown material and reference sample, while they are being applied to a controlled temperature. Figure 2.1 shows differential scanning calorimeter device supplied by Netzsch, and Table 2.1 displays the typical data for sapphire, a base material used in this study. Technical Specifications of the DSC 200 F3 Maia® is given in Table 2.2.

Table 2.1

Typical data of DSC [11]

Test Specimen	Temperature, T, °C	Specific heat capacity, C_p, J/g°C
Standard Sapphire	26.85	0.7788
	36.85	0.7994
	46.85	0.8188
	56.85	0.8373
	66.85	0.8548



Figure 2.1 Netzsch Differential Scanning Calorimeter

Table 2.2

Technical Specifications of the DSC 200 F3 Maia®

Technical Specifications Netzsch DSC	
Temperature Range	-170 °C to 600 °C
Heating Rates	0.001 K/min to 100 K/min
Cooling Rates	0.001 K/min to 100 K/min
Sensor	Heat flux system
Temperature Accuracy	0.1 K
Enthalpy accuracy	< 1%

Netzsch differential scanning calorimeter device is commonly used to measure specific heat capacity of material as defined by ASTM E-1269 standard [12]. The technique can also determine how a material's heat capacity varies with respect to temperature. Figure 2.2 describes Netzsch DSC cross section view of the device. To perform specific heat capacity experiment, a test specimen and reference sample is placed on a metallic pan with high thermal conductivity within the calorimeter. The metallic pan must ensure good heat conduction between

the sample and reference. The sample and the reference are subjected to a certain temperature. The calorimeter measures the temperature difference and calculates heat flow.

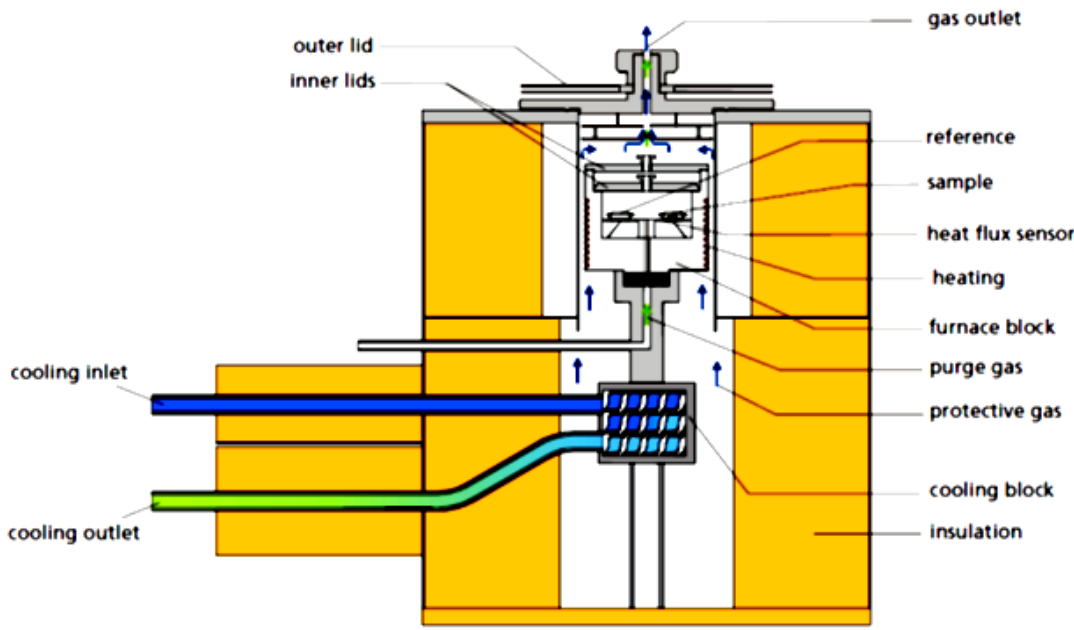


Figure 2.2 Netzsch DSC Cross Section View

Heat flow rate and the heating rate of the sample is measured using the differential scanning calorimeter, and then the measured data is used to calculate specific heat capacity of the unknown specimen based on the following analysis:

The specific heat capacity of a material at constant pressure is given is given by Equation 2.2

$$C_p = \frac{1}{m} \frac{dQ}{dT} \quad (2.2)$$

where m is the mass of the material and, $\frac{dQ}{dT}$ is the gradient of the heat flow rate with respect to temperature T .

The Equation 2.2 can be written as:

$$C_p = \frac{1}{m} \frac{dT}{dt} \frac{dQ}{dt} \quad (2.3)$$

Or

$$C_p = \frac{\left(\frac{dQ}{dt} \right)}{m \left(\frac{dT}{dt} \right)} \quad (2.4)$$

Because the precise measurement of $\frac{dQ}{dt}$ and $\frac{dT}{dt}$ are very difficult to measure and depends on equipment, a machine constant (E_M) is established with a (C_p) of known material. Here Indium is used as a reference material and (E_M) is established for Netzsch DSC equipment. Then the specific heat (C_p) of unknown material is calculated by:

$$C_p = \frac{\left(\frac{dQ}{dt} \right)}{m \left(\frac{dT}{dt} \right)} E_M \quad (2.5)$$

The machine constant (E_M) was calculated from the separate test using the same equipment by the following equation

$$E_M = \frac{m \left(\frac{dT}{dt} \right)}{\left(\frac{dQ}{dt} \right)} C_p \quad (2.6)$$

The experiment was conducted by setting the machine from T_0 temperature to T_{\max} with a set heating rate $\frac{dT}{dt}$. Then the heat flow rate $\frac{dQ}{dT}$ is measured at different temperatures. The measured machine constant (E_M) at 20 °C (room temperature) found to be 0.284, and it varied from 0.284 to 0.287 for a temperature ranging 20°C 100°C. The specific heat

capacity is independent of specimen size and shape, but the sample should be small enough to maintain the uniform temperature throughout the mass.

2.4 Measurement of Thermal Diffusivity (α)

Thermal diffusivity is the measurement of how quickly heat can transfer through a material. It plays a great role in the performance of materials especially high temperature applications and determines the working temperature levels of the material. It is important to study and analyze thermal diffusivity of a material because it plays significant role in determination of safe operating temperature, design of thermal systems, and process control parameters. The thermal diffusivity (α) is measured as per the ASTM Standard E-1461

The thermal diffusivity can be determined in many different ways. Numerous methods have been used to measure thermal diffusivity such as the Flash method [13], Thermographic methods [2], Thermal Wave Interferometry (TWI) [3], and others. But the most common technique used to measure the thermal diffusivity is the Anter Flashline 2000 method. Figure 2.3 displays Flashline 2000 Thermal Properties Analyzer. Tables 2.3 and 2.4 display technical specifications and the thermal diffusivity data for reference (thermographite) material.



Figure 2.3 Flashline 2000 Thermal Properties Analyzer

Table 2.3

Technical Specifications of the Flash Line TM 2000 Thermal Properties Analyzer

Technical Specifications of Netzsch DSC	
Pulse Source:	High Speed Xenon Discharge
Thermal Diffusivity Range:	0.001 – 10 cm ² /s
Operating Temperature Range:	Room Temperature to 330°C
Furnace	Heat flux system
Atmosphere	Air or Inert Gas Purge
Testing Samples	1 – 6 mm thick, 6 – 30 mm diameter
Cooling Options	Nitrogen

Table 2.4

Typical data of thermal diffusivity of thermographite [14]

Test Specimen	Temperature, T, °C	Thermal diffusivity α_3, cm²/s
Thermographite	25	0.0026
	50	0.0025
	75	0.0023
	100	0.0023
	125	0.0022
	150	0.0021

Flash method for measuring thermal diffusivity was developed in 1961 by W. J. Parker [15]. This method is widely used in many countries. It is considered a standard method of measuring the thermal diffusivity of materials. The flash method can be used to measure the thermal diffusivity of small thin cylindrical specimen is heated between 20 and 100°C, using laser or lamp as the energy source. When the furnace has reached the specific temperature, the

front face of the specimen is subjected to quick radiant energy pulse and a detector measures the resulting temperature change between the front and rear faces (see Figure 2.4). The specimen the temperature between the two faces is monitored till the (ΔT) becomes constant with time. The time required for ΔT to reach $\frac{\Delta T}{2}$ is recorded as half time. The half time and the specimen thickness (L in meter) are used in parker Equation 2.7 to calculate to calculate the thermal diffusivity (α) of the material.

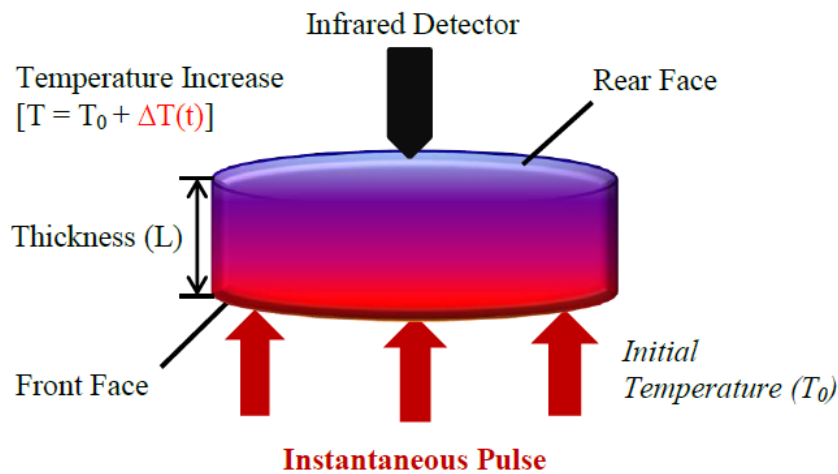


Figure 2.4 Schematic of the Flash Method

$$\alpha = \frac{1.37}{\pi^2} \left(\frac{L^2}{t_{1/2}} \right) \quad (2.7)$$

According to ASTM 1461 the test is valid if $t_{1/2}$ falls between 10 and 1000 ms

Parker's model considered ideal condition that is the specimen is very thin, homogeneous and no radiation loss. A number of researchers have developed correction to Parker's Equation 2.7. The one found to be simple, accurate and incorporated in Anter Flash equipment is The Clark and Taylor [16] correction factor E_{C-T} , which account the radiation heat

loss. The correction factor is calculated by taking $t_{0.25}$ and $t_{0.75}$ times for $\frac{\Delta T}{4}$ and $\frac{3\Delta T}{4}$ respectively, using the Equation 2.8.

$$E_{C-T} = -0.3461467 + 0.361578 \left(\frac{t_{0.75}}{t_{0.25}} \right) - 0.0652543 \left(\frac{t_{0.75}}{t_{0.25}} \right)^2 \quad (2.8)$$

Then the material diffusivity is given by

$$\alpha_{corrected} = \frac{L^2}{t_{1/2}} E_{C-T} \quad (2.9)$$

The correction decrease the value of (α) from α_p

2.5 Validation of Methodology

The measured specific heat (C_p) in this research is 0.8979 J/g°C. The measured Axial (α_1) and transverse (α_3) thermal diffusivity are 3.9×10^{-2} cm²/s and 5.4×10^{-3} cm²/s respectively. The calculated axial (k_1) and transverse (k_3) conductivities are 4.95 W/mK and 0.6915W/mK respectively. All these values were obtained at room temperature which considered reasonable and accurate results compared with literature data lists in Table 2.5.

Table 2.5

Thermal properties of carbon- carbon composite at room temperature [17]

Property	Carbon- Carbon
Specific heat, C_p , J/g,°C	0.9433
Axial diffusivity, α_1 , cm ² /s	0.0245
Transverse diffusivity, α_3 , cm ² /s	0.0066
Axial conductivity, k_1 , W/mK	3.77
Transverse conductivity, k_3 , W/mK	1.01

2.6 Laminate and Specimens Preparation for Unidirectional Composites

Fiber reinforced composite materials have different thermal properties in different directions [1]. Unidirectional composites made from prepreg that can be classified as orthotropic material, the principal directions are along the fiber and across the fiber as in Figures 2.5 and 2.6. Thermal properties in x_2 and x_3 directions are equal. Therefore, by selectively preparing the specimen, one can measure axial and transverse thermal diffusivity of the material. Since the density (ρ) and specific heat (C_p) are scalar they do not change with direction. Only the diffusivity (α) changes with direction, which can be measured by Anter Flash method as used following ASTM E-1461 test standard. The fiber and across the fiber directions are represented by x_1 and x_2 (x_3) axes respectively. The properties in x_2 and x_3 directions are one and same, so we can measure the thermal properties in x_3 direction. Figure 2.5 and 2.6 shows how the specimens were cut from the unidirectional laminate to measure transverse (α_3) and axial (α_1) diffusivities of the composite, respectively. The specimen's diameter is 12.5 mm, and the thicknesses are 3mm and 1mm for the axial and transverse diffusivity measurement, respectively. Details of specimen's preparation and testing are presented in chapter 4.

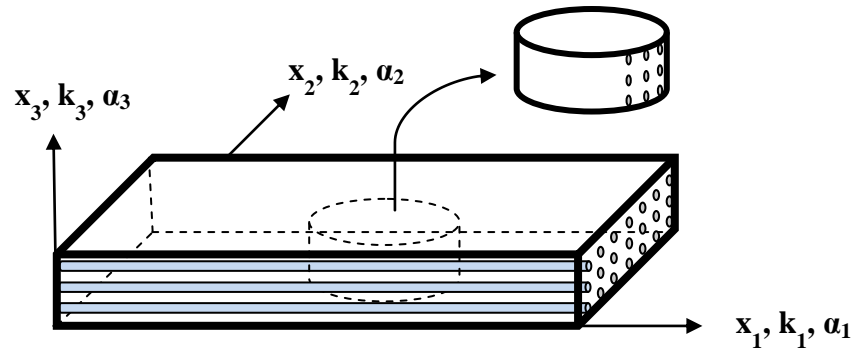


Figure 2.5 Principal directions of unidirectional composites and specimens extraction for transverse diffusivity measurement

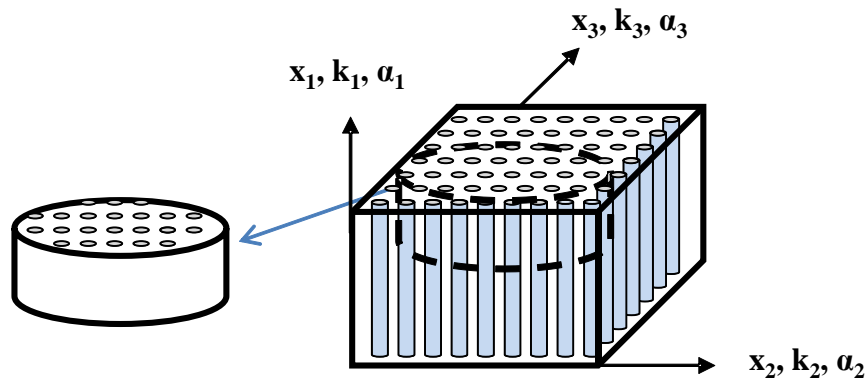


Figure 2.6 Principal directions of unidirectional composites and specimens extraction for axial diffusivity measurement

2.7 Summary

Thermal conductivity determination involves measurement of thermal diffusivity, specific heat capacity, and the specimen density. Thermal diffusivity of composite material can be measured using Anter Flashline 2000 Thermal Properties Analyzer by properly extracting the specimen from the unidirectional composite, and specific heat capacity can be measured using Netzsch differential scanning calorimeter. The relevant data and the associated equipment are

summarized. The ASTM E-1461 and ASTM E-1269 standards can be followed to measure the thermal diffusivity and specific heat, respectively.

CHAPTER 3

AS4/3501-6 Carbon/Epoxy Composite Material Samples Preparation

3.1 Introduction

This chapter describes the preparation of AS4/3501-6 carbon/Epoxy laminates. The fabrication process includes prepreg cutting, stacking, debulking, molding, and specimens cutting. The first set of the specimens were prepared to be tested through the thickness of the laminate in (x_3) direction. The second set was prepared to be tested through axial (x_1) diffusivity measurement. Polishing and optical imaging of the prepared specimens also described in this chapter.

3.2 Fabrication of Panels

Two laminate panels, one with 152.4 mm X 152.4 mm X 0.75 mm, and the other with 76.2 mm X 76.2 mm X 20 mm sizes of AS4/3501-6 carbon/Epoxy unidirectional composite material was fabricated using autoclave process at the Center of Composite Material Research (CCMR) Laboratory at North Carolina A&T State University. Figure 3.1 shows the photograph of prepreg used for fabricated laminates. The fiber volume fraction of the laminated composite was calculated using the formula:

$$V_f = \frac{A_f N}{10^3 \rho_f h} \quad (3.1)$$

where V_f is the fiber volume fraction, A_f is the fiber areal weight (g/m^2), N is the numbers of plies in the laminate, ρ_f is fiber density (g/cm^3), and h is laminate thickness (mm). Properties of the laminates are listed in Table 3.1. The calculated fiber volume fractions are 67 % and 64 % for the thin and thick laminates, respectively.

Table 3.1

Fabricated AS4/3501-6 carbon/Epoxy material properties [18]

Physical Properties	AS4/3501
Fiber areal weight, g/m ²	150
Fiber density, g/cm ³	1.79
Thin laminate fiber volume fraction, %	67
Thick laminate fiber volume fraction, %	64
Resin content, %	33



Figure 3.1 AS4/3501-6 composite prepreg for laminates fabrication

3.3 Preparation Specimen for Diffusivity Test

A unidirectional laminated composite is an assembly of two or more layers of unidirectional fibers oriented at same direction that is compacted and cured [1]. The laminated material properties are defined with respect to the orientation of the fibers in the lamina. The

three principal directions of the lamina are x_1 , x_2 , and x_3 as shown in Figure 3.2. The x_1 is the fiber direction and x_2 and x_3 represent perpendicular to the fiber directions. Properties in x_2 and x_3 are same or (isotropic), therefore the determination of the conductivity in x_3 and x_1 directions are sufficient to get all three dimensional properties of the laminate.

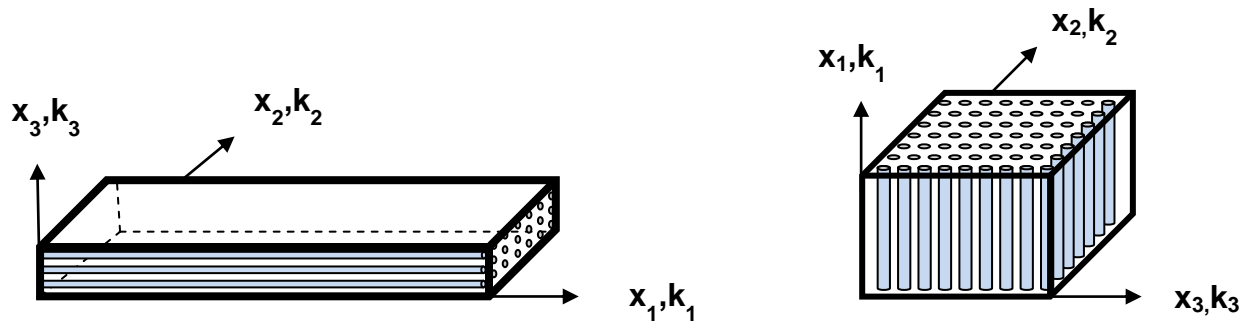


Figure 3.2 The principal directions of laminated composite material

3.4 Specimens Preparation for Diffusivity Measurement

Two types of cylindrical specimen were prepared from the two laminates. The thin laminate (152.4 mm X 152.4 mm X 0.75 mm) was for through the thickness diffusivity measurement and (76.2 X 76.2 mm X 20 mm) thick laminate for axial measurement. Five cylindrical specimens of 12.5 mm diameter were cut from thin laminate drilled by a core cutter drill that is rotating at 200 RPM (see Figure 3.3).

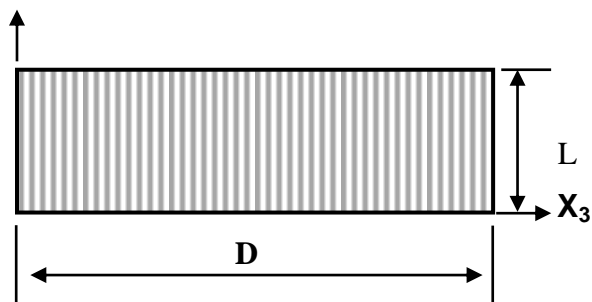
Each of the specimens was hand sanded on top and bottom faces by 600 hand paper to take out the mold release coat. Then all the specimens were cleaned in an Ultrasonic bath. The dimensions of axial specimens were measured and density of the material was calculated. The specimen number, diameter, length and the density of axial and transverse specimen are listed in Table 3.2. Figure 3.4 and 3.5 shows the specimen geometry and photography axial and transverse diffusivity measurement specimens, respectively.



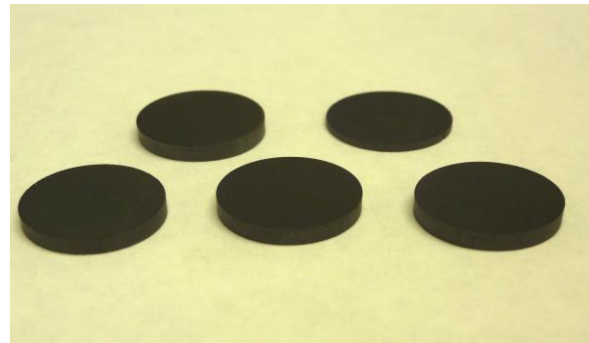
Figure 3.3 Drilling machine used to cut AS4/3501-6 composite laminate

Five specimens were prepared for diffusivity measurement through axial direction as shown in Figure 3.4, and Table 3.2 describes the physical Properties of the specimens. In this table, the specimen number represent by Sp-A or Sp-T, where ‘Sp’ stand for specimen, ‘T’ for transverse direction, and ‘A’ fiber axial fiber direction. The ‘#’ goes from 1 to 5.

x_1



(a) Axial specimen geometry



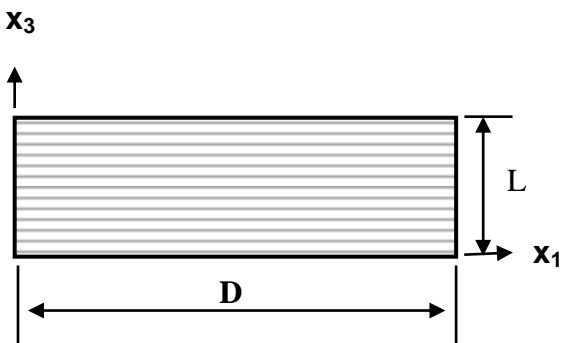
(b) Specimen photograph

Figure 3.4 Axial specimen geometry and photograph

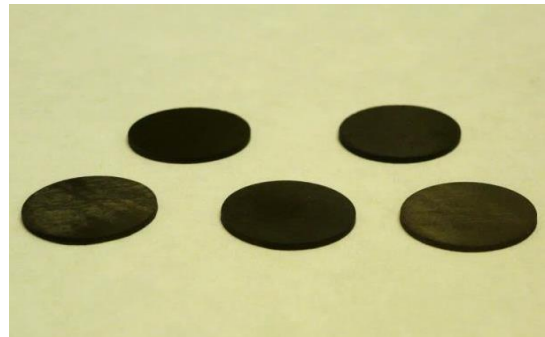
Table 3.2

Specimen for axial diffusivity (α_1) measurement.

Test Specimen	Diameter, D, mm	Thickness, L, mm	Mass, m, g	Density, ρ , g/cm ³
Sp-A-1	12.67	2.93	0.522	1.42
Sp-A-2	12.61	2.94	0.531	1.42
Sp-A-3	12.54	2.95	0.522	1.42
Sp-A-4	12.62	2.95	0.527	1.41
Sp-A-5	12.63	2.96	0.531	1.42



(a) Transverses specimen geometry



(b) Specimen photograph

Figure 3.5 Model and photograph of through the thickness diffusivity measurement.

Table 3.3

Specimen for transverse diffusivity (α_3) measurement.

Test Specimen	Diameter, D, mm	Thickness, L, mm	Mass, m, g	Density, ρ , g/cm ³
Sp-T-1	12.59	0.728	0.130	1.43
Sp-T-2	12.78	0.728	0.133	1.42
Sp-T-3	12.65	0.738	0.132	1.41
Sp-T-4	12.67	0.744	0.134	1.41
Sp-T-5	12.66	0.748	0.133	1.40

3.5 Specimen Preparation for Specific Heat Test

The specific heat capacity of the material is scalar independently specimen geometry and size. A representative volume of the composite material was selected for measurement of the specific heat (C_p). Five cylindrical specimens 4 mm in diameter and 1 mm thickness were prepared (see Figure 3.6). Each specimen was tested separately for certain range of temperature (22 °C to 100 °C) then the specific heat was calculated. Table 3.4 lists the specimen diameter and thickness for all specimens prepared.

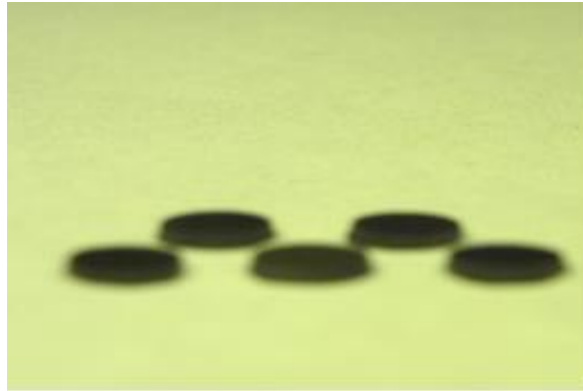


Figure 3.6 Specimens prepared for specific heat capacity test

Table 3.4

Physical Properties of Specimens for specific heat capacity test

Test Specimen	Diameter, D, mm	Thickness, L, mm	Mass, m, g
Sp-1	3.86	0.774	0.013
Sp-2	3.88	0.773	0.014
Sp-3	3.93	0.824	0.014
Sp-4	3.92	0.823	0.013
Sp-5	3.87	0.774	0.013

3.6 Optical Microscopy of the Specimen

To assure proper orientation of the fiber and directionality of the diffusivity measurement typical specimen shown in Figure 3.7 was polished on the x_1-x_3 and x_2-x_3 planes. Then the optical images were taken to confirm the fiber alignment. Polishing was performed by Buehler Polisher using different sand papers. The advanced Nikon eclipse LV150 microscope was used for optical imaging of the specimen shown in Figure 3.8.

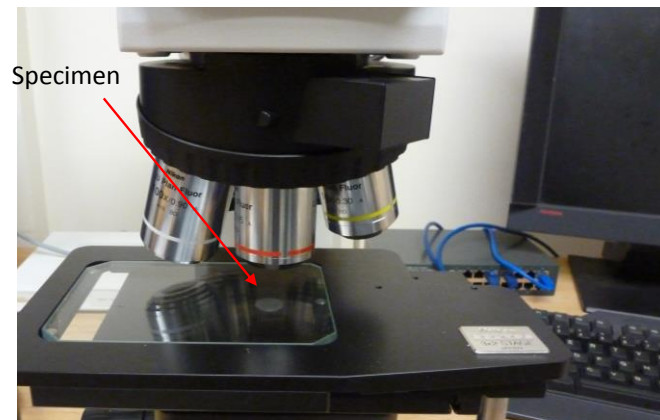


Figure 3.7 Nikon eclipse LV150 microscope

Figure 3.8 displays the material orientation and top surface x_1-x_2 microscopic image of the thin specimen used for transverse diffusivity (α_3) measurement. Note the fibers are parallel to each other and perpendicular to x_1-x_2 planes. The Figure 3.9 displays image top view of the specimen used for axial diffusivity (α_1) measurement. The specimen was prepared from the thick laminate. The microscopic images were taken at different magnification, circular, cross-section of the fiber indicate that the x_2-x_3 planes is perpendicular to the axial direction of the fiber. This kind of accuracy of the specimen preparation is required accurate measurement of diffusivity in different directions.

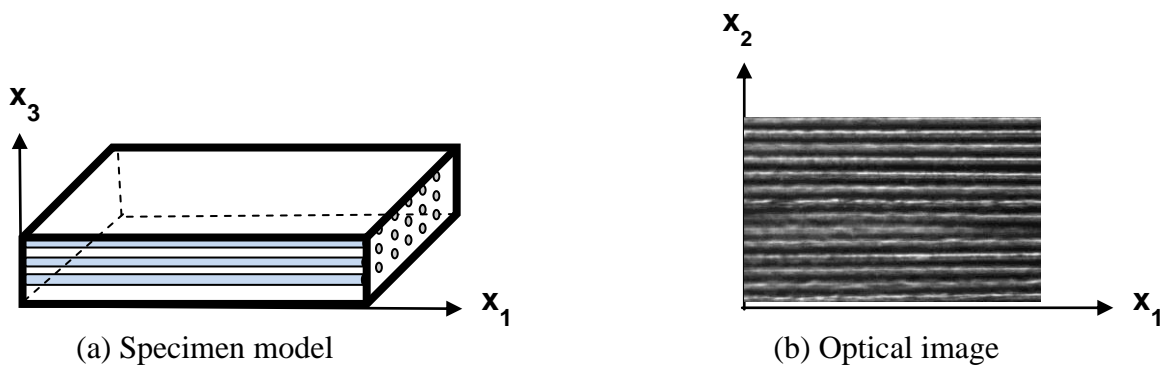


Figure 3.8 Thin specimen (through –the – thickness) measurement model and optical image of the specimen on $x_1 - x_2$ plane

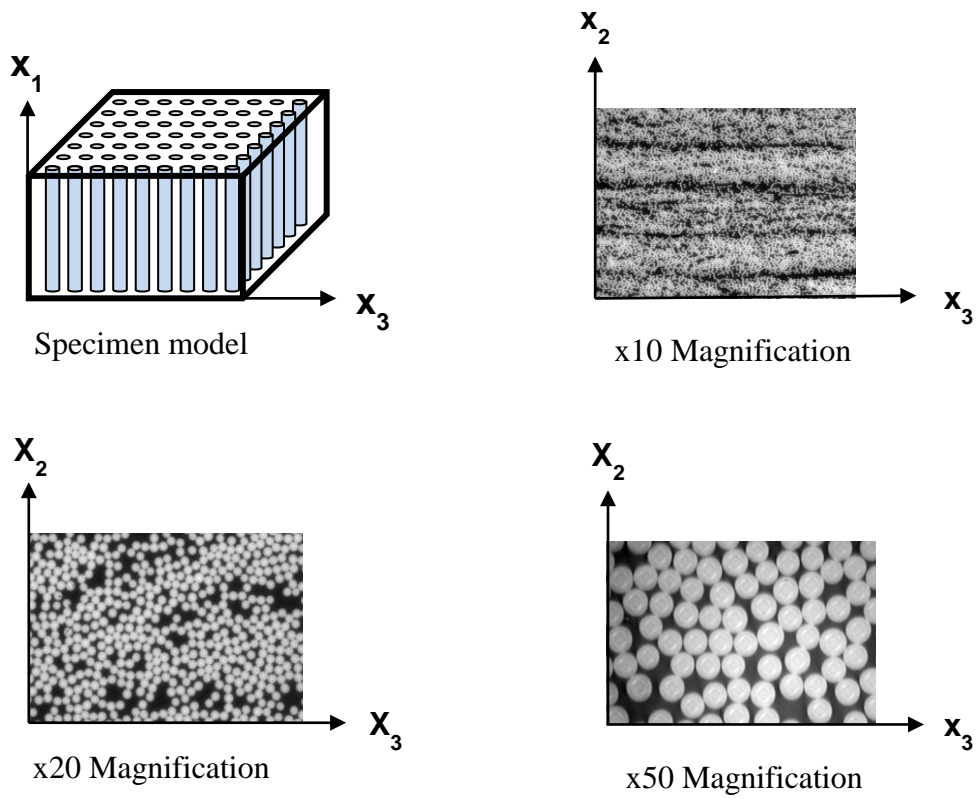


Figure 3.9 Thick specimen (axial measurement) model and optical images of $x_2 - x_3$ plane at 10, 20 and 50 magnifications.

3.7 Special Test Studies

Two special tests studies were made. Namely, specimen thickness affect (thicknesses 2 mm and 3 mm), and specimen surface coating with and without graphite powder. Additional specimens were prepared for these test studies.

3.8 Summary

Unidirectional AS4/3501-6 composite laminate was fabricated and used for test specimen preparation. Two sets of specimens were prepared:

The thick laminate for axial conductivity (k_1) measurement and the thin laminate for through - the - thickness (k_3) conductivity measurement. Optical image of specimen showed the orthogonal orientation of fiber to measure axial and transverse diffusivity of the composite. The specimen nominal diameter and length (thickness) were 12.5 mm and 3 mm respectively, for axial test; and 12.5 mm and 0.75 mm for transverse test. Typical mass of specific heat specimen was about 0.013g.

CHAPTER 4

Experiments and Results

4.1 Introduction

This chapter explains in details the experimental procedure used to measure orthogonal thermal diffusivity properties using flash method technique and then the specific heat capacity using Netzsch Differential scanning calorimeter (DSC) for AS4/3501-6 unidirectional composite laminate. The measured data will be used to calculate thermal conductivity in axial and transverse directions of the unidirectional AS4/3501-6 composite laminate. Five specimens were tested and then the average values at room temperature were compared with the literature.

4.2 Measurement of Specific Heat Capacity (C_p)

As explained in chapter 2 that Netzsch Differential scanning calorimeter (DSC) was used to measure specific heat capacity of AS4/3501-6 laminated composite material specimens. The DCS test was conducted following the guidelines in the ASTM E-1269 standard test method for measuring specific heat capacity. The DSC measures the temperature difference and calculates heat flow from the input data for a reference sample or material. In the test Indium was used as a standard for calibration [19]. Five test samples of thin cylindrical of diameter 4 mm and mass about 0.013 were used for measuring the specific heat capacity (C_p) of AS4/3501-6 composite laminate.

4.2.1 Test preparation. The test started with turning on the Data acquisition system and DSC 200 F3 Maia® device. The argon gas valve was turned on with 40 ml/min flow rate to allow the system to be purged. Aluminum pans were used as specimen holders during the tests. Using tweezers, two empty pans were placed on the heat flux sensor to run the base line test. The empty pans were centered the sample and reference locations. The furnace was heated to room

temperature (22 °C), and held at least for five minutes while the calorimeter recorded the thermal data. After the baseline run completed, the calorimeter testing chamber was cooled to ambient temperature. The pan on reference location was replaced with a sapphire and the previous baseline run was applied to correct for the aluminum pan. After the sapphire run completed, the actual test sample was placed on the right side of the chamber as shown in Figure 4.1 and the same temperature program was used to complete the experiment.



Figure 4.1 Top view of specimen placed on the heat flux Sensor [20]

4.2.2 Test procedure and data. The DCS test was conducted from room temperature (22 °C) to 100 °C, at heating rate of 10 °C/min and the data collect the data at interval about 10 °C. The table 4.1 (column 1) lists the test temperature sampling. At each temperature, the specimen was held about 5 minutes to maintain the isothermal condition. The data acquisition system provided the specimen specific heat at the specified temperature based on the Equation 2.5. The table 4.1 lists the specific heat capacity (C_p) of all specimens from 22 °C to 99 °C. The average and standard deviation (STD) of the five specimens are listed in the last two columns. The Figure 4.2 shows the plot of specific heat capacity (C_p) against temperature for all five specimen (hollow symbols), and the average (solid circle). Least regression fit through the average values flow the linear equation:

$$C_p = 0.844 + 3.50 \times 10^{-3} T \quad (4.1)$$

with the R value 0.993.

Table 4.1

Specific heat capacity (C_p) results of AS4/3501-6 carbon/Epoxy

Temperature, $T, ^\circ\text{C}$	Specific Heat, $C_p, \text{J/g}^\circ\text{C}$					Average	Standard deviation, σ
	Sp #1	Sp #2	Sp #3	Sp #4	Sp #5		
22	0.9203	0.9017	0.8913	0.8571	0.9192	0.898	0.026
29	0.9719	0.9478	0.938	0.9103	0.9713	0.948	0.026
38	1.0148	0.9832	0.9736	0.9508	1.0138	0.987	0.027
46	1.0529	1.0123	1.0044	0.9853	1.0517	1.021	0.030
57	1.0905	1.0399	1.0332	1.0171	1.0893	1.054	0.034
68	1.1281	1.0667	1.0606	1.0502	1.1262	1.086	0.038
78	1.1633	1.0942	1.0897	1.0817	1.1623	1.118	0.041
89	1.2008	1.1228	1.1172	1.1154	1.1992	1.151	0.045
99	1.2378	1.1511	1.1482	1.1491	1.2363	1.185	0.048

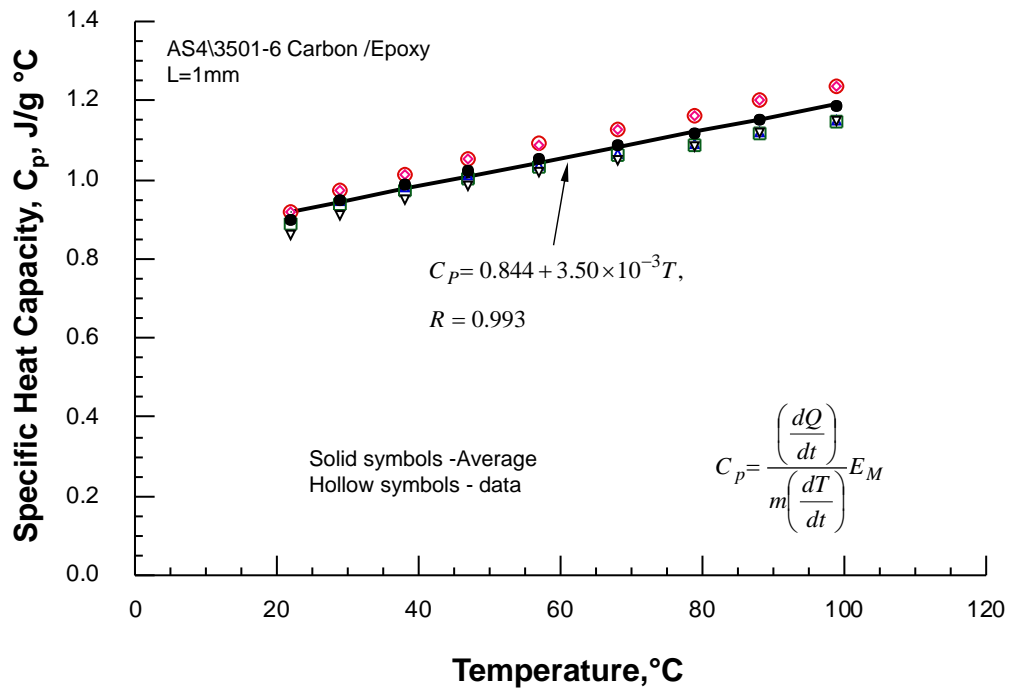


Figure 4.2 Specific heat capacity plot of tested specimens

As the testing temperature increases, the specific heat of the specimens continuously increases linearly from 0.844 J/g °C at 0°C at a rate of 3.5×10^{-3} per °C. Statistical analysis of the average and the standard deviation are given below:

$$\sigma = \sqrt{\frac{1}{N-1} \sum_{i=1}^N (a_i - a)^2} \quad (4.2)$$

Where, σ is the samples standard deviation and N is the total number of measurement.

The Standard Error (SE) was calculated for each temperature using standard deviation of the average, as shown below

$$SE = \frac{STD}{\sqrt{N-1}} \quad (4.3)$$

Normal distribution based on 95% confidence is 1.96, and the confidence interval error (e) is determined by the following:

$$e = \pm 1.96 \times SE \quad (4.4)$$

The percent error can be calculated by:

$$error = \frac{e}{mean} \times 100 \% \quad (4.5)$$

Finally the specific heat capacity (C_p) equation can be given by:

$$C_p = C_{p,ave.}(T) \pm e(T) \quad (4.6)$$

Table 4.2 shows the obtained calculated errors for specific heat and standard deviation for the corresponding temperature values, and Figure 4.3 displays the plot of the data. Circles represent the average value and the error bars represent the errors from Equation 4.4. Specific heat

increases with the temperature, it follows nearly linear curve. The error varies between 2.7% to 4% based on 95% confidence.

Table 4.2

Specific heat capacity results of AS4/3501-6 carbon/Epoxy

Temperature, T, °C	Average Specific Heat, $C_{p\text{avr.}}$, J/g, °C	Standard Deviation, σ	Standard Error, SE	Percent Error, e (%)
22	0.8979	0.0259	0.0129	2.8
29	0.9479	0.0256	0.0128	2.7
38	0.9872	0.0274	0.0137	2.7
47	1.0213	0.0299	0.0150	2.9
57	1.0540	0.0338	0.0169	3.1
68	1.0864	0.0377	0.0189	3.4
79	1.1183	0.0409	0.0205	3.6
88	1.1511	0.0447	0.0224	3.8
99	1.1845	0.0480	0.0240	4.0

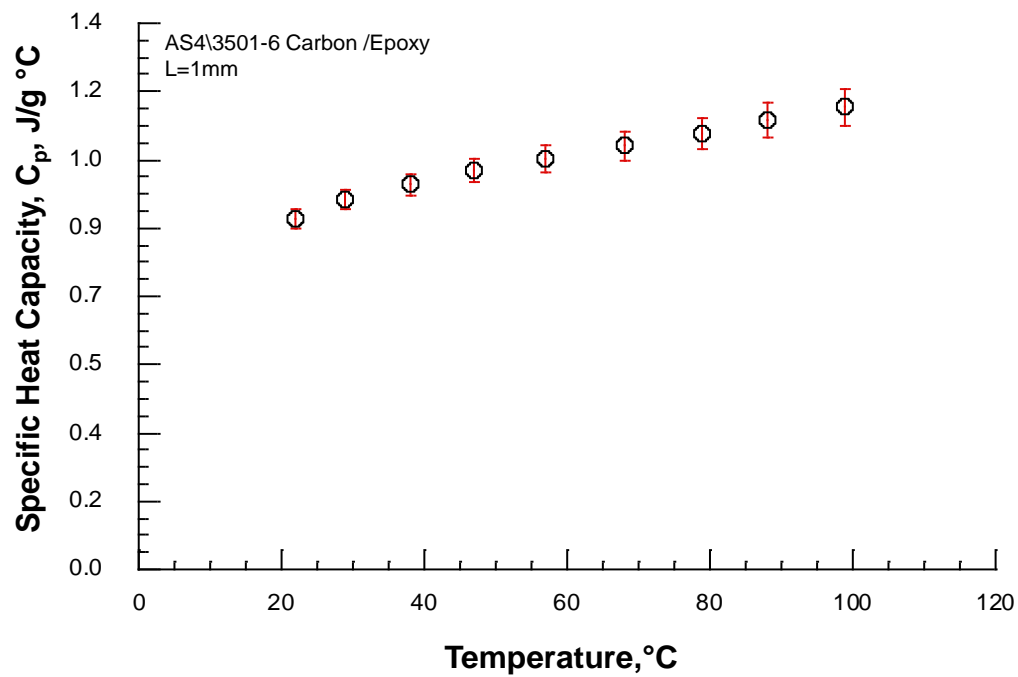


Figure 4.3 Average specific heat capacity and its error

4.3 Measurement of the Thermal Diffusivity (α)

The Flash line 2000 Thermal Properties Analyzer was used to measure thermal diffusivity of the composite laminated samples. Thermal diffusivity of 4 specimens were measured first and followed by 5th specimen. The technique was followed ASTM E-1461 test standard it used 12.5 mm (0.5 inch) diameter cylindrical composite material samples. Figure 4.4 shows Block Diagram of a Flash System with data acquisition and analysis software.

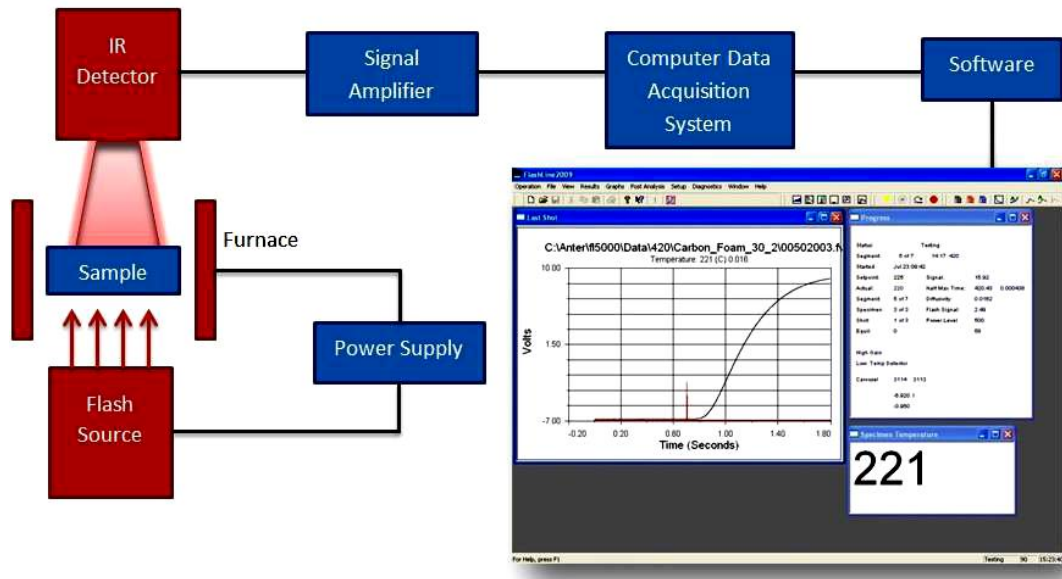


Figure 4.4 Block diagram of the Flash line 2000 Thermal Properties Analyzer

The Flash line 2000 Thermal Properties Analyzer consist of specimen holder, laser flash source, temperature response detector, recording device, and an environmental enclosure when testing above and below room temperature according to ASTM Standard E-1461. The flash source is laser that emits a quick energy pulse. The technique is a tabletop-based instrument that utilized a high temperature furnace which can heat the test room in ranging from

chamber temperature to 500 °C [21]. At first the diffusivity was measured according to Parker's equation (Equation 2.7) and then Clark and Taylor's thermal correction (Equation 2.8) was applied to minimize the radiation effect. The sample changer allowed 4 samples positions that can moved automatically into the measurement positions controlled by the software. Figure 4.5 shows a picture of the actual equipment.

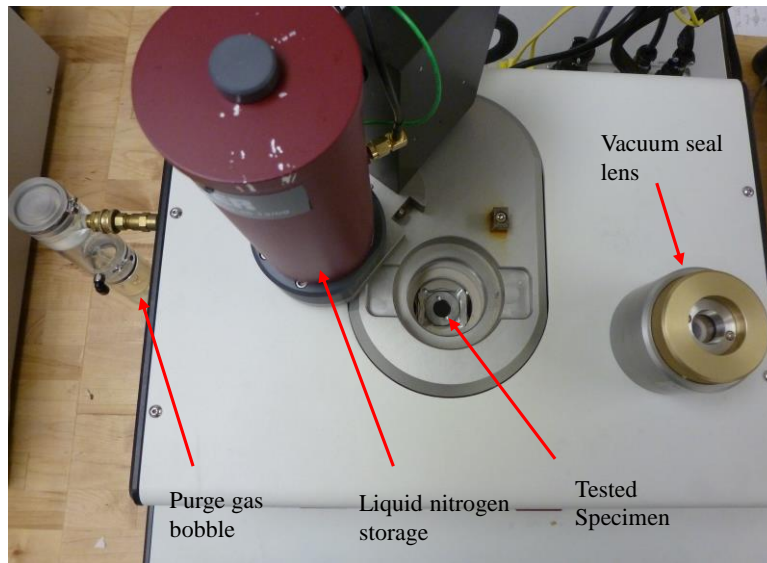


Figure 4.5 Photo graph of top view of Flash line 2000 Thermal Properties Analyzer

4.3.1 Software setup. The Flashline 2000 software was started by double clicking on its icon on the data acquisition system. Then the test temperature values, number of segments (9 segment), number of shots per segment (3 shots), and voltage setting were entered. After the experiment completed, the window showed a summary of the test data.

4.3.2 Testing. The specimen was placed in the test chamber using the sample's tweezers and the nitrogen gas valve was opened the appropriate nitrogen cylinder after making sure that there is enough nitrogen gas in the cylinder. Also the safety check valve is open to allow for nitrogen gas flow. Nitrogen gas flow was verified visually by inspecting the flow indicator on the furnace for bubbles in the oil. The pressure indicator on the nitrogen gas tank was 5 psi. Liquid

nitrogen used because it has ability to create a fast cooling process and prevent the IR detector from overheating.

4.3.3 Axial thermal diffusivity (α_1). One of the beauties of the present test approach is by properly orienting the fiber in the composite different directional conductivity can be measured. The axial samples shown in Figure 3.5 were tested to measure the axial diffusivity (α_1). Tables 4.3 through 4.5 lists the diffusivities values of five test samples from room temperature 22 °C to 100 °C. In the Table, the specimen thickness (L), half time ($t_{1/2}$) Parker diffusivity (α_{1p}), and the Clark – Tylor corrected diffusivity (α_1) were listed. Figure 4.6 illustrates the plot of the axial thermal diffusivity (α_1) of AS4/3501-6 against temperature. All the specimen data and average value of each temperature shown. Solid circles represent the average value. The least square regression Equation of (α_1) is given by:

$$\alpha_1 = 0.04 - 5 \times 10^{-5} T \quad (4.7)$$

The R value of curve is 0.96.

As the testing temperature increases the axial diffusivity (α_1) decreases, it follows nearly linear curve. The error varies between 2.1% to 4.9% based on 95% confidence.

Table 4.3

Axial thermal diffusivity (α_1) of Sp #1 and Sp #2

Temperature, T, °C	Sp #1, L= 2.93 mm			Sp #2, L= 2.94 mm		
	Half time $t_{1/2}$, s	Diffusivity α_{1p} , cm ² /s	Corrected Diffusivity, α_1 , cm ² /s	Half time $t_{1/2}$, s	Diffusivity α_{1p} , cm ² /s	Corrected Diffusivity, α_1 , cm ² /s
22	0.3079	0.0387	0.0385	0.3149	0.0381	0.0378
29	0.3063	0.0389	0.0386	0.3199	0.0375	0.0372
38	0.3063	0.0389	0.0386	0.3199	0.0375	0.0372
46	0.3229	0.0369	0.0366	0.3191	0.0376	0.0373
57	0.3169	0.0376	0.0374	0.3251	0.0369	0.0367
68	0.3161	0.0377	0.0374	0.3368	0.0350	0.0347
78	0.3169	0.0376	0.0374	0.3314	0.0362	0.0359
89	0.3186	0.0374	0.0372	0.3389	0.0354	0.0351
99	0.3203	0.0372	0.0370	0.3428	0.0350	0.0347

Table 4.4

Axial thermal diffusivity (α_1) of Sp #3 and Sp #4

Temperature, T, °C	Sp #3, L= 2.95 mm			Sp #4, L= 2.95 mm		
	Half time $t_{1/2}$, s	Diffusivity α_{1p} , cm ² /s	Corrected Diffusivity, α_1 , cm ² /s	Half time $t_{1/2}$, s	Diffusivity α_{1p} , cm ² /s	Corrected Diffusivity, α_1 , cm ² /s
22	0.3247	0.0372	0.0370	0.3020	0.0400	0.0398
29	0.3256	0.0371	0.0368	0.3081	0.0392	0.0390
38	0.3089	0.0391	0.0389	0.3179	0.0380	0.0377
46	0.3491	0.0346	0.0343	0.3238	0.0373	0.0371
57	0.3129	0.0386	0.0384	0.3291	0.0367	0.0365
68	0.3300	0.0366	0.0364	0.3412	0.0354	0.0352
78	0.3522	0.0343	0.0340	0.0343	0.0352	0.0350
89	0.3447	0.0350	0.0348	0.3607	0.0335	0.0333
99	0.3487	0.0346	0.0344	0.3706	0.0326	0.0324

Table 4.5

Axial thermal diffusivity (α_1) of Sp #5

Temperature, T, °C	Sp #5, L= 2.96 mm		
	Half time $t_{1/2}$, s	Diffusivity, α_{1p} , cm ² /s	Corrected Diffusivity, α_1 , cm ² /s
22	0.2966	0.0410	0.0408
29	0.3094	0.0393	0.0391
38	0.3397	0.0358	0.0356
46	0.3217	0.0378	0.0376
57	0.3200	0.0380	0.0378
68	0.3332	0.0365	0.0363
78	0.3495	0.0348	0.0346
89	0.3537	0.0344	0.0342
99	0.3622	0.0336	0.0334

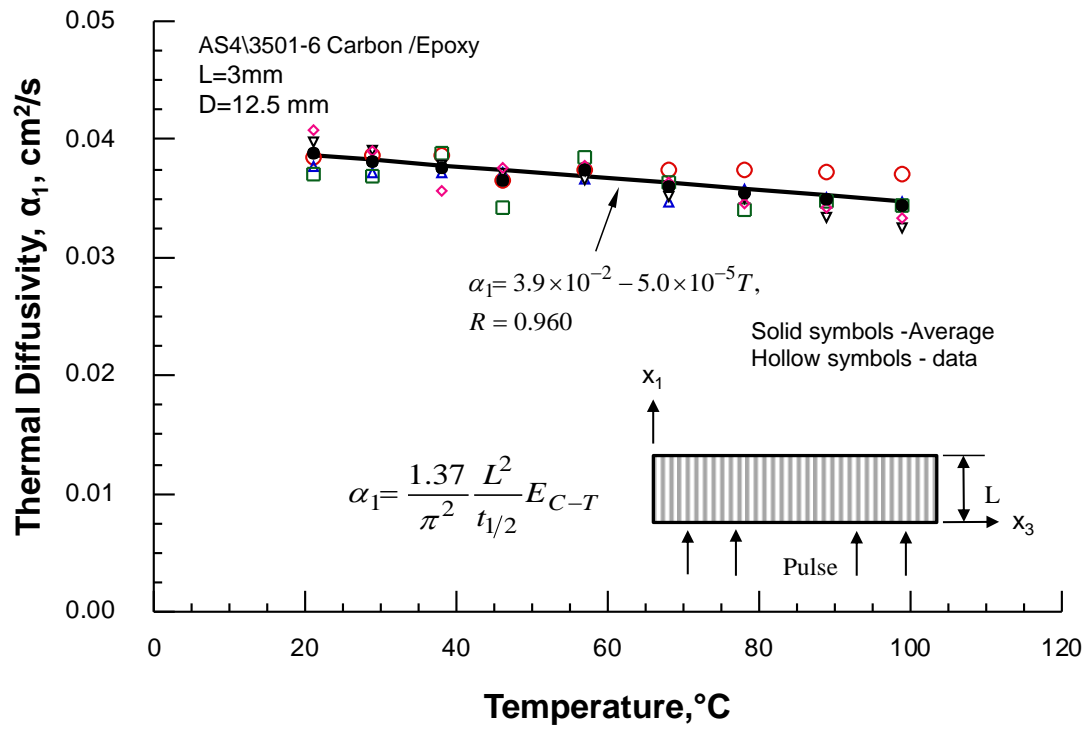


Figure 4.6 The average axial thermal diffusivity (α_1)

Table 4.6

Percentage error of the thermal the axial diffusivity (α_1)

Temperature, T, °C	Average Diffusivity, α_1 , cm ² /s	Standard Deviation, σ	Standard Error, SE	Percent Error, e, (%)
22	0.0387	0.0015	0.0008	3.9
29	0.0383	0.0011	0.0005	2.7
38	0.0378	0.0013	0.0007	3.4
47	0.0374	0.0013	0.0007	3.5
57	0.0369	0.0008	0.0004	2.1
68	0.0363	0.0011	0.0005	2.9
79	0.0358	0.0013	0.0007	3.6
88	0.0353	0.0015	0.0007	4.1
99	0.0348	0.0017	0.0009	4.9

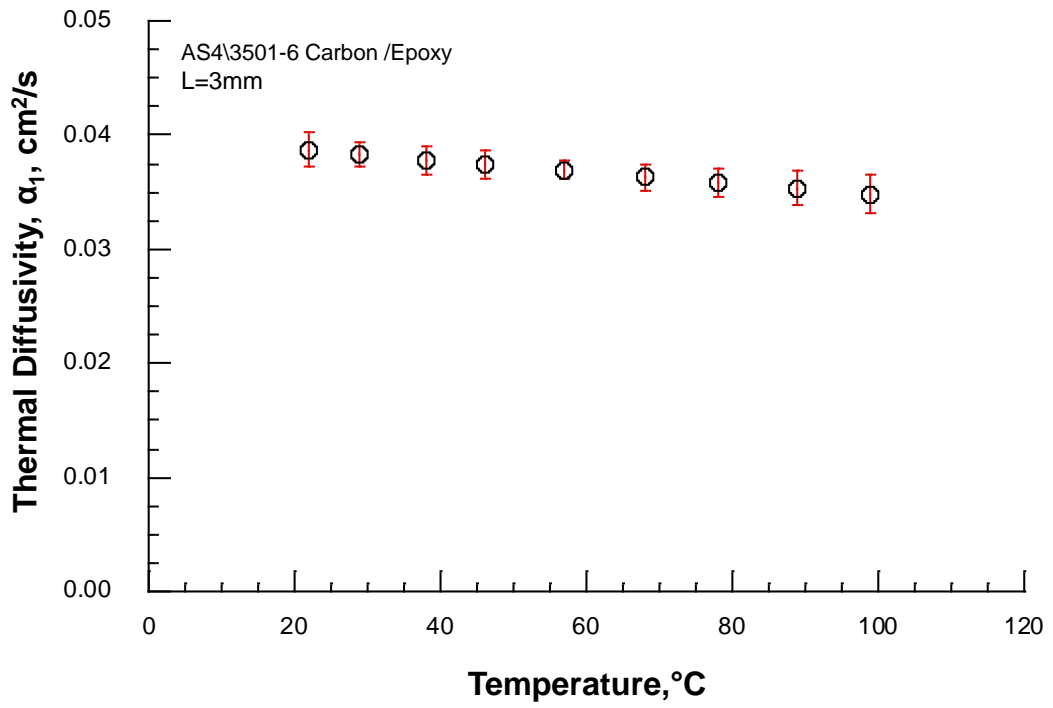


Figure 4.7 The average axial diffusivity with its standard deviation

4.3.4 Transverse thermal diffusivity (α_3). Transverse diffusivity (α_3) was also measured by Anter Flashline 2000 Thermal Properties Analyzer, in which the flash laser was applied perpendicular to the fiber direction (on x_3 direction of the composite laminate). Tables 4.7 through 4.9 lists the diffusivity (α_3) values at temperatures from 22 °C to 99 °C and Figure 4.8 illustrates the plot of transverses thermal diffusivities (α_3). As the testing temperature increases the transverse diffusivity (α_3) decreases, it follows linear curve. The error varies between 1.6% and 2.9% based on 95% confidence.

Table 4.7

Transverse thermal diffusivity data of Sp #1 and Sp #2

Temperature, T, °C	Sp #1, L= 0.728 mm			Sp #2, L= 0.728 mm		
	Half time, $t_{1/2}$, s	Diffusivity α_{3p} , cm ² /s	Corrected Diffusivity, α_3 , cm ² /s	Half time, $t_{1/2}$, s	Diffusivity, α_{3p} , cm ² /s	Corrected Diffusivity, α_3 , cm ² /s
22	0.1314	0.0056	0.0053	0.1268	0.0058	0.0055
29	0.1337	0.0052	0.0052	0.1268	0.0058	0.0055
38	0.1337	0.0052	0.0052	0.1268	0.0058	0.0055
46	0.1362	0.0054	0.0051	0.1291	0.0057	0.0054
57	0.1362	0.0054	0.0051	0.1314	0.0056	0.0054
68	0.1388	0.0053	0.0050	0.1314	0.0056	0.0053
78	0.1442	0.0051	0.0049	0.1337	0.0055	0.0052
89	0.1442	0.0051	0.0049	0.1388	0.0053	0.0050
99	0.1471	0.0050	0.0048	0.1415	0.0052	0.0049

Table 4.8

Transverse thermal diffusivity data of Sp #3 and Sp #4

Temperature, T, °C	Sp #3, L= 0.738 mm			Sp #4, L= 0.744 mm		
	Half time, $t_{1/2}$, s	Diffusivity, α_{3p} , cm ² /s	Corrected Diffusivity, α_1 , cm ² /s	Half time, $t_{1/2}$, s	Diffusivity, α_{3p} , cm ² /s	Corrected Diffusivity, α_1 , cm ² /s
22	0.1374	0.0055	0.0053	0.1372	0.0056	0.0054
29	0.1400	0.0054	0.0052	0.1372	0.0056	0.0054
38	0.1402	0.0054	0.0052	0.1397	0.0055	0.0053
46	0.1416	0.0054	0.0052	0.1397	0.0055	0.0053
57	0.1426	0.0053	0.0051	0.1423	0.0054	0.0052
68	0.1436	0.0053	0.0051	0.1423	0.0054	0.0052
78	0.1454	0.0052	0.0050	0.1450	0.0053	0.0051
89	0.1482	0.0051	0.0049	0.1450	0.0053	0.0051
99	0.1512	0.0050	0.0048	0.1478	0.0052	0.0050

Table 4.9

Transverse thermal diffusivity data of Sp #5

Temperature, T, °C	Sp #5, L= 0.748 mm		
	Half time, $t_{1/2}$, s	Diffusivity, α_{3p} , cm ² /s	Corrected Diffusivity, α_3 , cm ² /s
22	0.1339	0.0058	0.0056
29	0.1339	0.0058	0.0056
38	0.1362	0.0057	0.0055
46	0.1362	0.0057	0.0055
57	0.1387	0.0056	0.0054
68	0.1387	0.0056	0.0054
78	0.1412	0.0055	0.0053
89	0.1438	0.0054	0.0052
99	0.1553	0.0050	0.0048

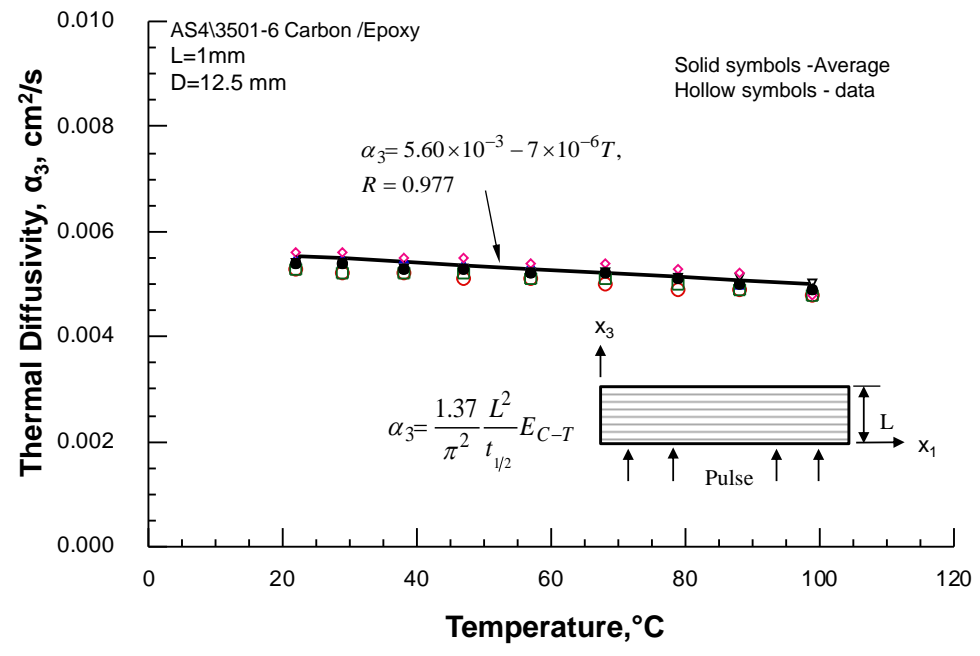


Figure 4.8 The average transverse thermal diffusivity

Table 4.10 shows the results for the transverse thermal diffusivity and standard deviation for the corresponding temperature values, and Figure 4.9 displays the pots.

Table 4.10

The results for the transverse thermal diffusivity and standard deviation

Temperature, T, °C	Average Diffusivity, α_3 , cm ² /s	Standard Deviation, σ	Standard Error, SE	Percent Error e (%)
22	0.0054	0.0001	0.0001	2.4
29	0.0054	0.0002	0.0001	2.9
38	0.0053	0.0002	0.0001	2.5
47	0.0053	0.0002	0.0001	2.6
57	0.0052	0.0002	0.0001	2.5
68	0.0052	0.0002	0.0001	2.7
79	0.0051	0.0002	0.0001	2.7
88	0.0050	0.0001	0.0001	2.3
99	0.0049	0.0001	0.0000	1.6

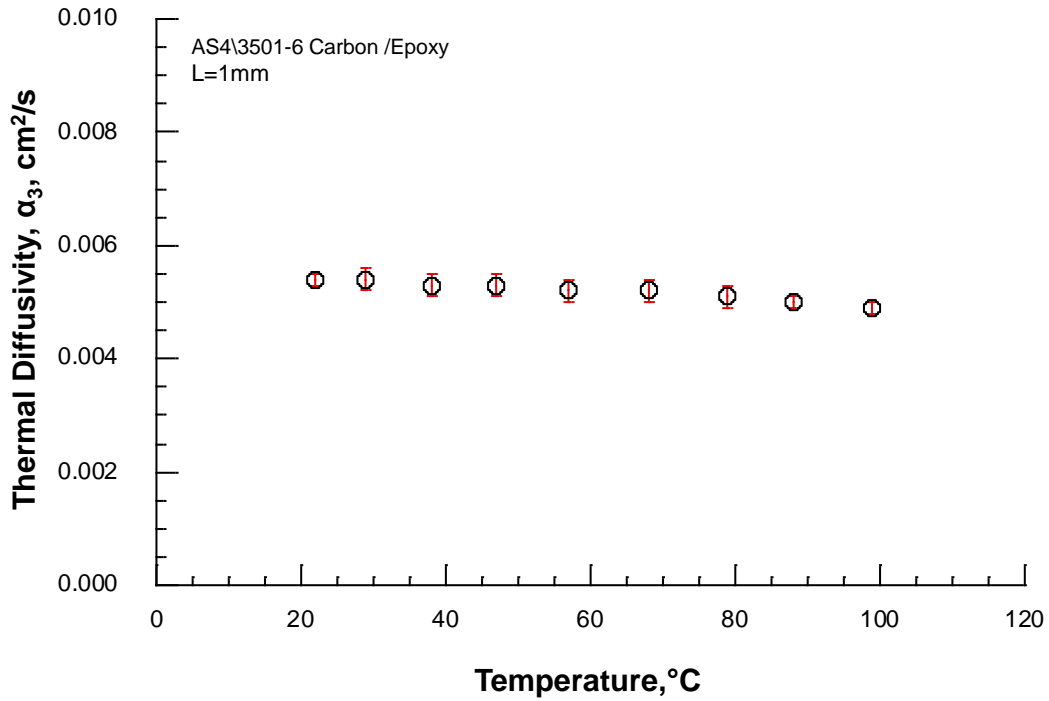


Figure 4.9 The Transverse diffusivity with its standard deviation

4.3.5 Summary. The measured Axial and transverse thermal diffusivity at room temperature were $3.9 \times 10^{-2} \text{ cm}^2/\text{s}$ (with 3.5% error) and $5.4 \times 10^{-3} \text{ cm}^2/\text{s}$ (with 2.1 % error) respectively. The transverse diffusivity reported in [8] was $4.6 \times 10^{-3} \text{ cm}^2/\text{s}$ which is nearly reasonable compared to present data ($5.4 \times 10^{-3} \text{ cm}^2/\text{s}$). In addition AS4/3501-6 Carbon/Epoxy diffusivity values are compared to IM78552-1 Carbon /Epoxy values carried out by Furkan Ulu (North Carolina A &T state University), and his results were $3.4 \times 10^{-2} \text{ cm}^2/\text{s}$ and $4.1 \times 10^{-3} \text{ cm}^2/\text{s}$ ($V_f = 0.58$), respectively.

4.4 Calculation of Thermal Conductivity (k)

Thermal conductivity is defined as ability of material to conduct heat. It is measured in Watts per square meter of surface area for a temperature gradient of 1 K per unit thickness of 1 m. By using the average density of five specimens, measured specific heat, and

thermal diffusivity, the thermal conductivity of the AS4/3501-6 composite was determined using the following relationship:

$$k = \rho \cdot C_p \cdot \alpha \quad (4.8)$$

The density is defined as mass divided by volume it can be calculated using the equation:

$$\rho = \frac{m}{V} \quad (4.9)$$

Where ρ is the density, m is mass, and V is the volume.

The results for the axial thermal conductivity of the AS4/3501-6 composite are shown in Table 4.11. There is a consistent increase in the thermal conductivity of the composite over the service temperature range it follows nearly linear curve as shown in Figure 4.10. Error values displays in table 4.12 and plodded in Figure 4.11.

Table 4.11

Calculated axial thermal conductivity (k_1) of specimens

Temperature, T, °C	Axial Conductivity k_1 , W/mK						Standard Deviation, σ
	Sp #1	Sp #2	Sp #3	Sp #4	Sp #5	Average	
22	4.9123	4.8229	4.7209	5.0781	5.2057	4.95	0.19
29	5.1991	5.0105	4.9566	5.2530	5.2664	5.14	0.14
38	5.4150	5.2186	5.4571	5.2888	4.9942	5.27	0.18
47	5.3118	5.4133	4.9780	5.3843	5.4569	5.31	0.19
57	5.6017	5.4968	5.7515	5.4669	5.6616	5.60	0.12
68	5.7735	5.3567	5.6191	5.4339	5.6037	5.56	0.16
79	5.9430	5.7046	5.4027	5.5616	5.4981	5.62	0.21
88	6.0881	5.7479	5.6988	5.4453	5.5909	5.71	0.24
99	6.2310	5.8473	5.7968	5.4517	5.6184	5.79	0.29

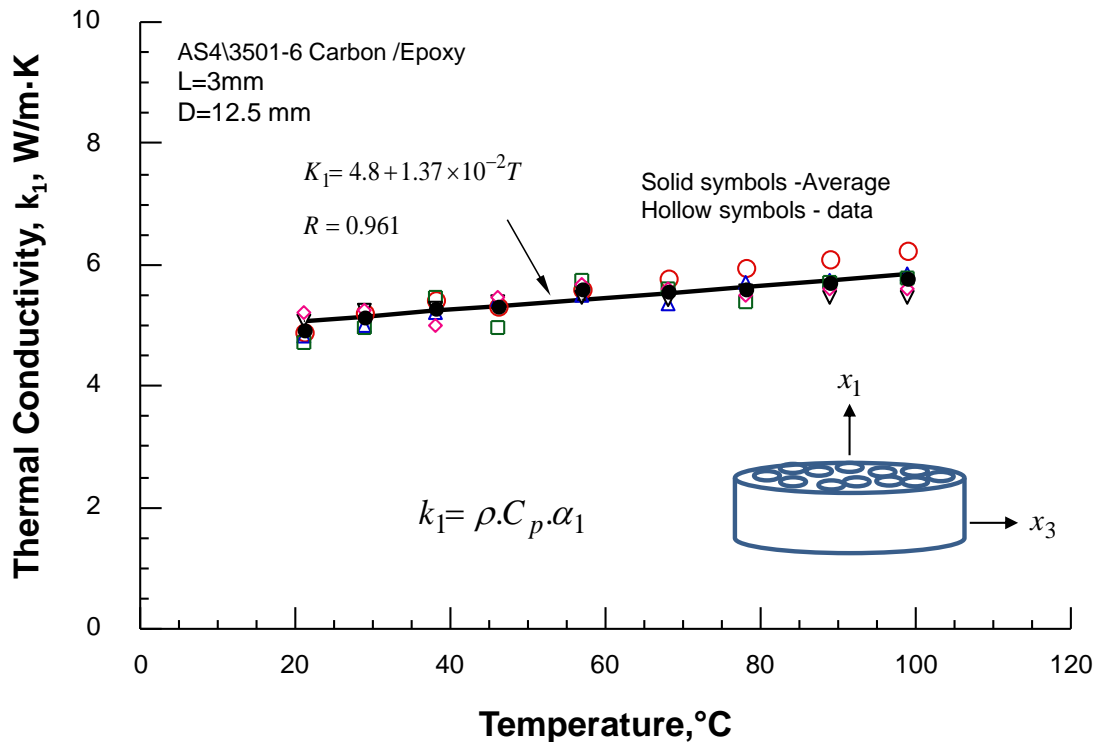


Figure 4.10 The Average axial thermal conductivity

Table 4.12

Calculated transverse thermal conductivity (k_3) of specimens

Temperature, T, °C	Transverse Conductivity k_3 , W/mK						Standard Deviation, σ
	Sp #1	Sp #2	Sp #3	Sp #4	Sp #5	Average	
22	0.6762	0.7018	0.6762	0.6890	0.7145	0.69	0.02
29	0.7004	0.7408	0.7004	0.7273	0.7543	0.72	0.02
38	0.7295	0.7716	0.7295	0.7435	0.7716	0.75	0.02
47	0.7402	0.7837	0.7547	0.7692	0.7982	0.77	0.02
57	0.7639	0.8088	0.7639	0.7788	0.8088	0.78	0.02
68	0.7719	0.8182	0.7873	0.8027	0.8336	0.80	0.02
79	0.7786	0.8263	0.7945	0.8104	0.8422	0.81	0.03
88	0.8015	0.8179	0.8015	0.8342	0.8506	0.82	0.02
99	0.8079	0.8247	0.8079	0.8416	0.8079	0.82	0.02

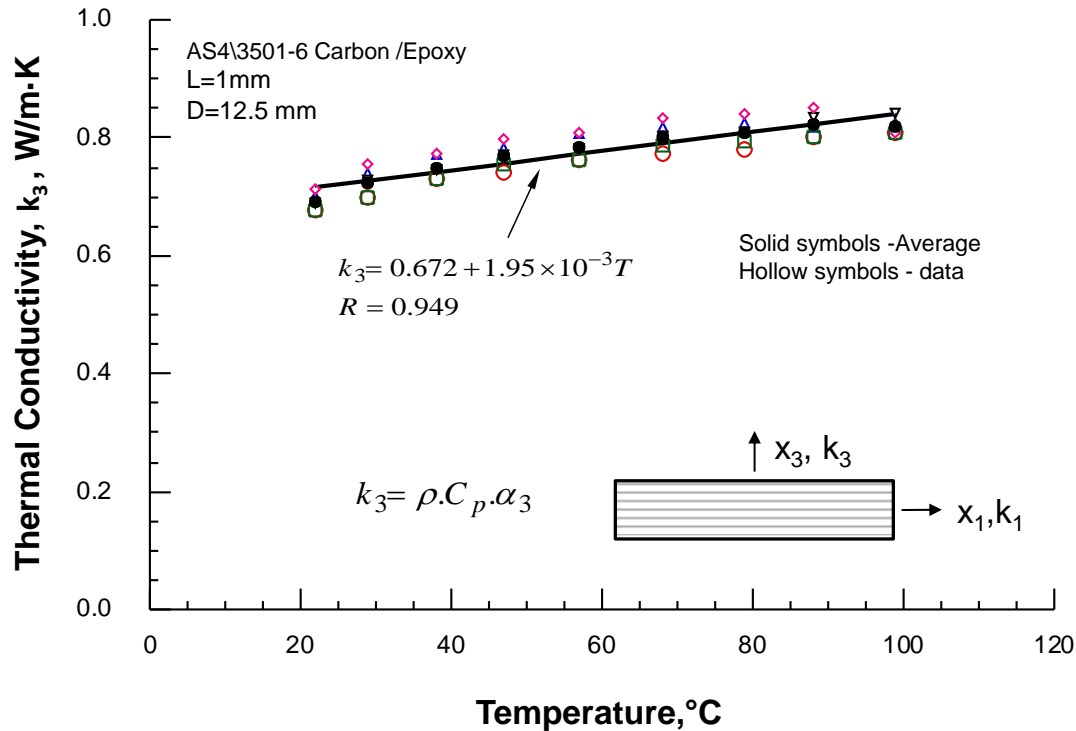


Figure 4.11 The average transverse thermal conductivity

4.5 Special Assessment

Two special cases were studied in this research regarding to the conductivity measurement of composite specimen. The first was the specimen thickness affect of the conductivity measurement. This was conducted on axial conductivity. The second was on surface coating of top and bottom faces of the specimen with graphite powder to improve surface emissivity.

4.5.1 The thickness affects. Test conducted before was for axial conductivity measurement for specimen thickness of about 3 mm. To determine the specimen thickness affect, the diffusivity of 2 mm thickness specimen was also measured, and listed in tables 4.13 through 4.15. The resulting diffusivity (α_1) was multiplied by specific heat capacity (C_p) (measured previously) and the density to calculate the conductivity (Equation 4.10). Table 4.16 lists the

conductivity for all five samples and the average for temperature ranging from 22 °C to 99 °C. The results were plotted as shown in Figure 4.12. Figure 4.12 illustrates the analysis of the results after reducing the thickness to 2mm.

$$k_1 = 4.8 + 1.61 \times 10^{-2} T \quad (4.10)$$

The R value of curve is 0.955.

Table 4.13

Axial thermal diffusivity (α_1) of Sp #1 and Sp #2

Temperature, T, °C	Sp #1, L= 2.05 mm			Sp #2, L= 2.00 mm		
	Half time $t_{1/2}$, s	Diffusivity α_{1p} , cm ² /s	Corrected Diffusivity, α_1 , cm ² /s	Half time, $t_{1/2}$, s	Diffusivity α_{1p} , cm ² /s	Corrected Diffusivity, α_1 , cm ² /s
22	0.1555	0.0375	0.0372	0.1438	0.0386	0.0383
29	0.1480	0.0394	0.0391	0.1413	0.0393	0.0390
38	0.1480	0.0394	0.0391	0.1442	0.0385	0.0381
46	0.1458	0.0400	0.0397	0.1457	0.0381	0.0378
57	0.1469	0.0397	0.0393	0.1391	0.0399	0.0397
68	0.1488	0.0392	0.0389	0.1420	0.0391	0.0388
78	0.1531	0.0381	0.0379	0.1442	0.0385	0.0382
89	0.1511	0.0386	0.0382	0.1492	0.0372	0.0369
99	0.1681	0.0347	0.0345	0.1525	0.0364	0.0361

Table 4.14

Axial thermal diffusivity (α_1) of Sp #3 and Sp #4

Temperature, T, °C	Sp #3, L= 2.01mm			Sp #4, L= 2.00 mm		
	Half time, $t_{1/2}$, s	Diffusivity, α_{1p} , cm ² /s	Corrected Diffusivity, α_1 , cm ² /s	Half time, $t_{1/2}$, s	Diffusivity α_{1p} , cm ² /s	Corrected Diffusivity, α_1 , cm ² /s
22	0.1460	0.0384	0.0382	0.1398	0.0397	0.0395
29	0.1423	0.0394	0.0390	0.1481	0.0375	0.0373
38	0.1326	0.0423	0.0421	0.1409	0.0394	0.0391
46	0.1545	0.0363	0.0360	0.1568	0.0354	0.0352
57	0.1566	0.0358	0.0356	0.1591	0.0349	0.0347
68	0.1507	0.0372	0.0370	0.1465	0.0379	0.0377
78	0.1553	0.0361	0.0358	0.1560	0.0356	0.0354
89	0.1532	0.0366	0.0364	0.1577	0.0352	0.0350
99	0.1487	0.0377	0.0375	0.1605	0.0346	0.0344

Table 4.15

Axial thermal diffusivity (α_1) of Sp #5

Temperature, T, °C	Sp #5, L= 2.03 mm		
	Half time, $t_{1/2}$, s	Diffusivity, α_{1p} , cm ² /s	Corrected Diffusivity, α_1 , cm ² /s
22	0.1437	0.0398	0.0396
29	0.1448	0.0395	0.0393
38	0.1409	0.0406	0.0404
46	0.1395	0.0410	0.0408
57	0.1412	0.0405	0.0403
68	0.1452	0.0394	0.0392
78	0.1402	0.0408	0.0406
89	0.1463	0.0391	0.0389
99	0.1419	0.0403	0.0401

Table 4.16

Axial thermal conductivity data for 2mm thickness

Temperature, T, °C	Axial Conductivity k_1 , W/mK					Average	Standard Deviation, σ
	Sp #1	Sp #2	Sp #3	Sp #4	Sp #5		
22	4.7464	4.8867	4.8740	5.0399	5.0526	4.8199	0.1278
29	5.2664	5.2530	5.2530	5.0240	5.2934	5.2179	0.1097
38	5.4852	5.3449	5.9060	5.4852	5.6675	5.5778	0.2163
47	5.7617	5.4859	5.2247	5.1086	5.9213	5.5004	0.3447
57	5.8863	5.9462	5.3321	5.1973	6.0360	5.6796	0.3854
68	6.0051	5.9896	5.7117	5.8198	6.0514	5.9155	0.1437
79	6.0225	6.0701	5.6888	5.6252	6.4515	5.9716	0.3326
88	6.2484	6.0358	5.9540	5.7250	6.3629	6.0652	0.2506
99	5.8069	6.0762	6.3118	5.7900	6.7494	6.1469	0.3994

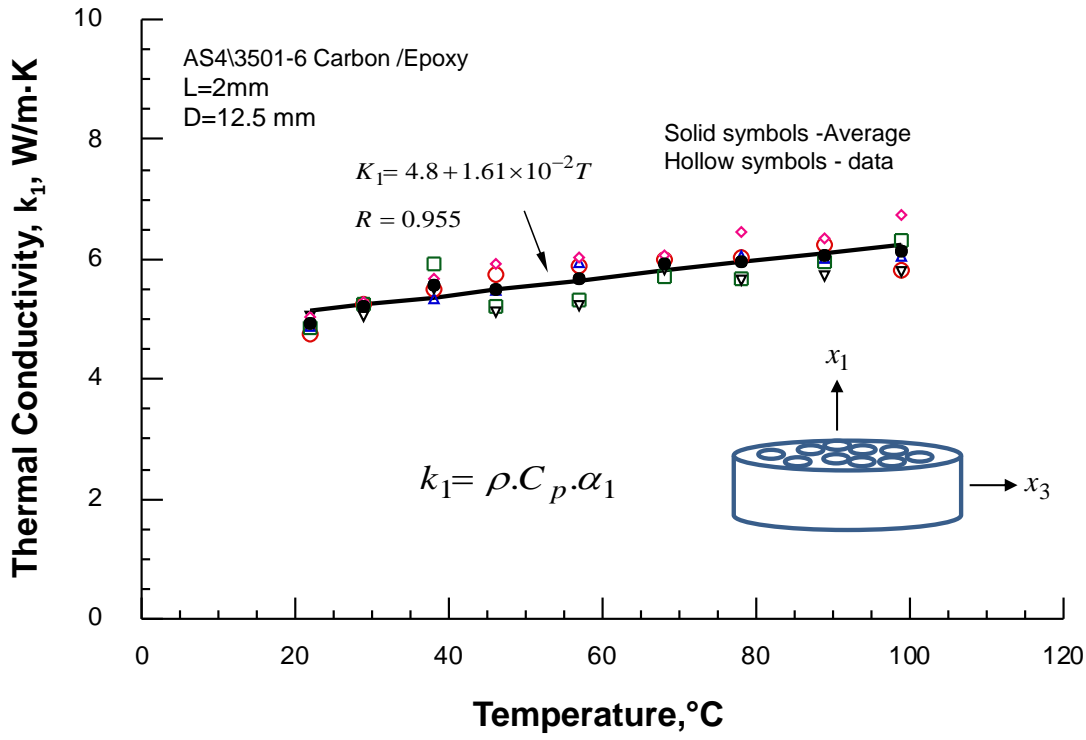


Figure 4.12 The average axial thermal conductivity for 2mm thickness

Figure 4.12 and a linear equation were fitted to the axial conductivity (k_l) using least square regression analysis, and the value of R was 0.955. The Figure 4.13 compares the average conductivity for 3mm and 2mm thickness samples. The error bar indicates the standard deviation. The two results agree with each other. Therefore the 3 mm specimen thickness was sufficient to measure the axial conductivity (k_l).

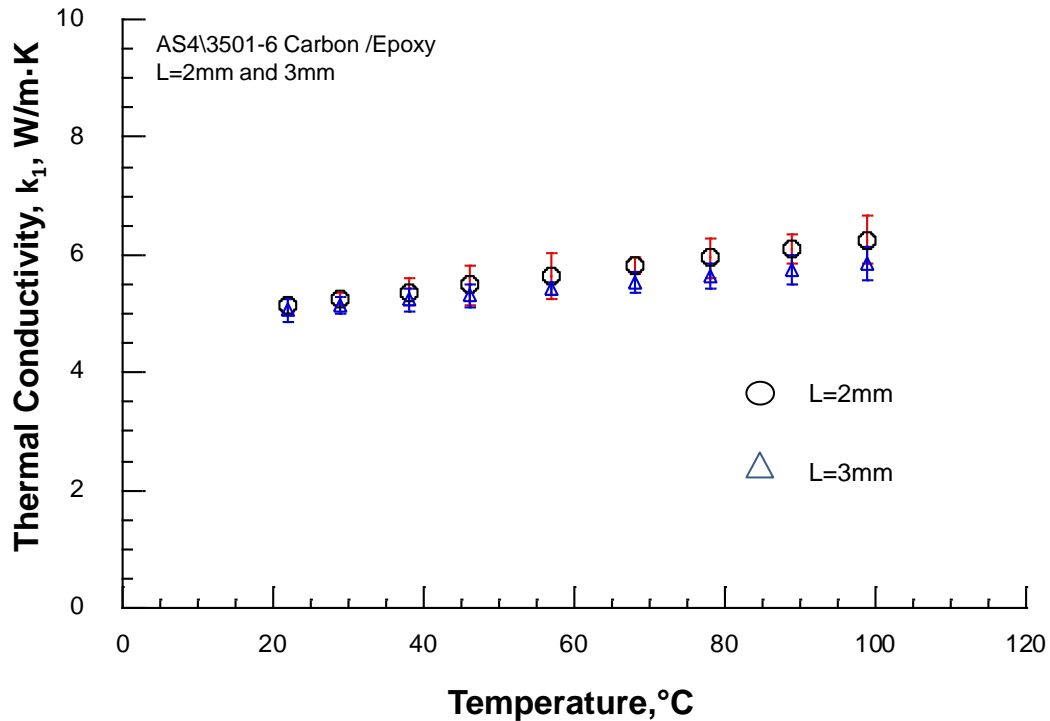


Figure 4.13 Comparison between the axial thermal conductivities for different thicknesses

4.5.2 Surface coating of specimen. Specimen surface coating by graphite powder was studied. Two separate diffusivity measurements were performed before coating and after coating top and bottom faces of the specimen by graphite powder. A 2mm specimen thickness in axial direction was selected. The specimen was tested without coating and then the surface was coated with graphite powder and tested again. The Table 4.17 listed axial conductivity (k_l) for coated and non-coated values at temperature range between 22 °C to 99 °C. The percent difference

varied from 2.8 at room temperature to 0.4% at 99 °C. This difference is within the data scatters of the test data (see Table 4.17). The Figure 4.14 displays the plot of the data for $22\text{ °C} \leq 99\text{ °C}$.

Table 4.17

Comparison of the axial thermal conductivity before and after coating

Temperature, T, °C	Axial Conductivity, k_1 , W/m°C		Percent Difference (%)
	Not Coated	Coated	
22	5.0526	5.1930	2.7778
29	5.2934	5.3068	0.2545
38	5.6675	5.7517	1.4851
46	5.8213	5.9213	1.7178
57	6.0360	5.8713	2.7295
68	6.0514	6.3447	4.8469
78	6.4515	6.5310	1.2315
89	6.3629	6.5592	3.0848
99	6.7494	6.7831	0.4988

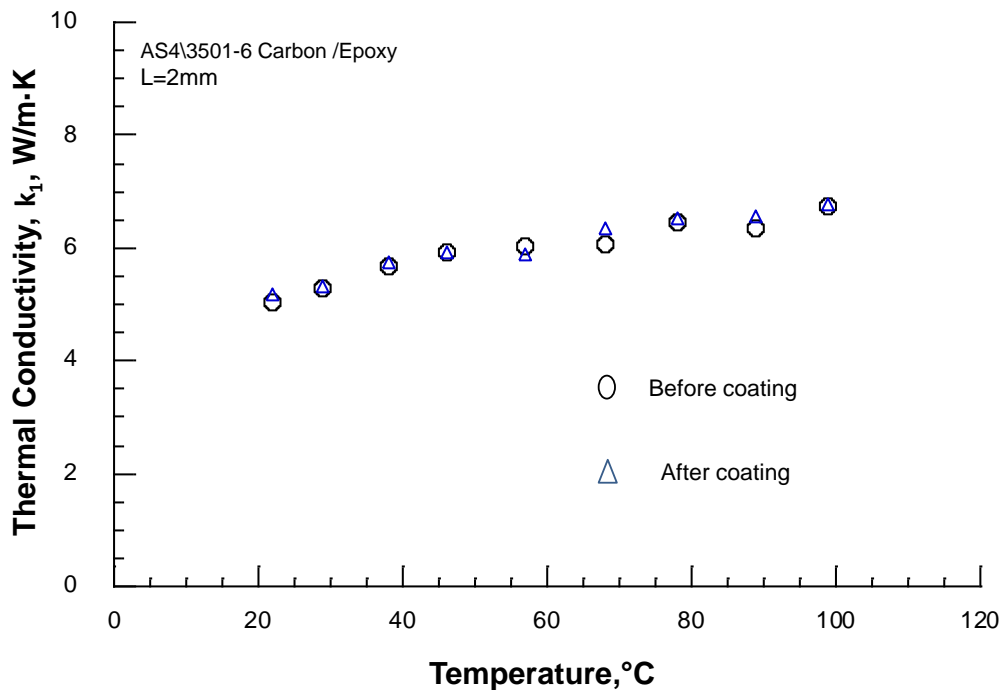


Figure 4.14 The axial thermal conductivity before and after coating

4.6 Summary

Netzsch Differential scanning calorimetry (DSC) device used to measure specific heat capacity of AS4/3501-6 composite laminates. Anter Flashline 2000 Thermal Properties Analyzer used to measure the thermal diffusivity. Proper preparation of the specimen in the axial as well as the transverse direction of the fiber enabled to get both axial and transverse thermal diffusivity and conductivity of the unidirectional carbon/epoxy composite. The test and data analysis resulted in linear equations as following:

$$\begin{aligned} 1. \text{ Specific heat } (C_p) \quad C_p &= 0.844 + 3.50 \times 10^{-3} T & (4.11) \\ R &= 0.993 \end{aligned}$$

$$\begin{aligned} 2. \text{ Axial diffusivity } (\alpha_1) \quad \alpha_1 &= 0.04 - 5 \times 10^{-5} T, & (4.12) \\ R &= 0.960 \end{aligned}$$

$$\begin{aligned} 3. \text{ Transverse diffusivity } (\alpha_3) \quad \alpha_3 &= 5.60 \times 10^{-3} - 7 \times 10^{-6} T, & (4.13) \\ R &= 0.977 \end{aligned}$$

$$\begin{aligned} 4. \text{ Axial conductivity } (k_1) \quad k_1 &= 4.8 + 1.37 \times 10^{-2} T, & (4.14) \\ R &= 0.961 \end{aligned}$$

$$\begin{aligned} 5. \text{ Transverse conductivity } (k_3) \quad k_3 &= 0.672 + 1.95 \times 10^{-3} T, & (4.15) \\ R &= 0.949 \end{aligned}$$

where T is the temperature in Celsius

All these equations were developed for temperature range of 20 °C (room temperature) to 100 °C, however the limited extrapolation of the equation from 0 °C to 125 °C will give reasonably accurate results. Note that in the above equation the temperature (T) is referenced from 0 °C. The room temperature thermal conductivity of AS4/3501-6 composite laminate $k_1=4.9$ W/mK and $k_3= k_2$ (because transverse isotropy material) = 0.69 W/mK for fiber

volume fraction (V_f) of 67%. The transverse conductivity of similar material (unknown V_f) testes by Bradley Dolemon [8] was 0.61 W/mK. The conductivity results of IM78552 carbon/epoxy composite $k_1=4.8$ W/mK and $k_2 = k_3 = 0.58$ W/mK.

CHAPTER 5

Thermal Conductivity Prediction by Micromechanics

5.1 Introduction

This chapter presents axial and transverse thermal conductivity prediction by micromechanics analysis. The axial conductivity (k_1) was obtained by rule of mixtures [22] while six models in literature were used to calculate the transverse conductivity (k_3). All models were compared with each other and the experimental data obtained in chapter 4.

5.2 Unit Cell Model

The unit cell model describes an idealized structure of the fiber reinforced composite assuming that the fiber is distributed in a square array. The unit cube describes the model of the structure. This was successfully used in literature to drive axial conductivity (k_1) using Equation 5.1, this model and various modifications were used to drive transverse conductivity (k_3) equations.

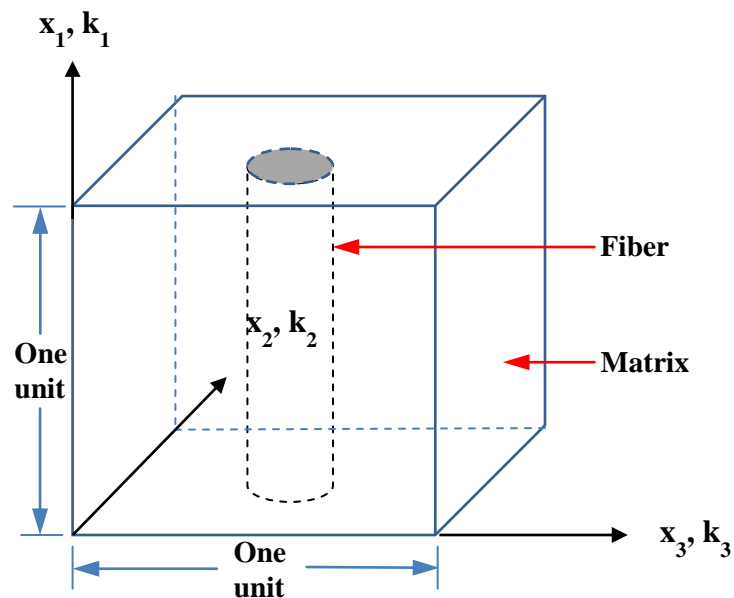


Figure 5.1 Description of the unit cell.

5.3 Axial Thermal Conductivity (k_1)

The axial thermal conductivity of a composite material can be calculated by rule of mixture (Equation 5.1) using the composite constituents of the material conductivity.

$$k_1 = V_f k_{1f} + V_m k_m \quad (5.1)$$

where k_1 , k_{1f} are the axial thermal conductivity of the composite and the fiber respectively, V_f is the fiber volume fraction, and k_m is the matrix conductivity.

Table 5.1 lists the constituent properties of AS4/3501-6 Graphite/Epoxy and AS4/3501-6 Carbon/Epoxy. The table also lists the fiber volume fraction (V_f) of both materials. The volume fractions are 0.64 and 0.67 for the axial and transverse conductivity, respectively. Calculated axial conductivity (k_1) from Equation 5.1 is 4.5 W/mK which agrees well with measured value of 4.9 W/mK in Chapter 4. The difference is less than 6% which is the same order as the test data scatter.

Table 5.1

Constituent properties of AS4 graphite/ epoxy and AS4/3501-6 composite material

Material	V_f		Thermal Conductivity, k , W/mK				
			Fiber	Matrix	Rule of mixture Eq (5.1)	Present	
	Axial	Transverse				Axial	Transverse
AS4/3501-6 Carbon/Epoxy [5, 23]	0.64	0.67	6.83	0.185	4.5	4.9	0.69
AS4.Graphite/Epoxy [7]		0.6	5.22	0.19			

5.4 Transverse Conductivity (k_3)

Computation of thermal conductivity through the thickness is more challenging than the axial conductivity. There are many assumptions made in derivation of conductivity from simple models [24]. Determining the matrix properties of the composite is usually simple and direct since this material can be fabricated in bulk form. On the other hand measuring the fiber properties in the transverse direction is more difficult comparing with the axial direction because of the small fiber size [7]. Because of the problems with direct measurement of fiber conductivity in transverse direction, matrix properties of the composite are measured and then the fiber properties are evaluated from the models. Several mathematical models have been developed to predict through the thickness thermal conductivity of composite material. These models assume that the fiber and matrix properties used the measured fiber volume fraction. Here, six models were used to calculate the transverse conductivity (k_3) of AS4/3501-6 composite laminate.

5.5 Models and Comparison

Below are six models which have been reported to predict of through the thickness thermal conductivity (k_3) as mentioned early. All of these models assume the knowledge of the fiber and the matrix conductivities and fiber volume fraction:

1. Chawla model:

$$k_3 = k_m \left(\left(1 - \sqrt{V_f} \right) + \frac{\sqrt{V_f}}{1 - \sqrt{V_f} \left(1 - \frac{k_m}{k_{3f}} \right)} \right) \quad (5.2)$$

2. Springer-Tsai model:

$$k_3 = k_m \left[\left(1 - 2\sqrt{\frac{V_f}{\pi}} \right) + \frac{1}{B} \left[\pi - \frac{4}{\sqrt{1 - \left(\frac{B^2 V_f}{\pi} \right)}} \tan^{-1} \frac{\sqrt{1 - \left(\frac{B^2 V_f}{\pi} \right)}}{1 + B\sqrt{\frac{V_f}{\pi}}} \right] \right] \quad (5.3)$$

where $B = 2 \left(\frac{K_m}{K_{3f}} - 1 \right)$

3. Hashin model:

$$k_3 = k_m + \frac{V_f}{\frac{1}{k_{3f} - k_m} + \frac{1 - V_f}{2km}} \quad (5.4)$$

4. Rayleigh model:

$$k_3 \approx k_m \left(1 - \frac{2V_f}{v' + V_f - \frac{C_1}{v'} V_f^4 - \frac{C_2}{v'} V_f^8} \right) \quad (5.1)$$

where $C_1 = 0.3058$, $C_2 = 0.0134$ and the expression for V' is given by

$$v' = \frac{\frac{km}{k_{3f}} + 1}{\frac{km}{k_{3f}} - 1} \quad (5.6)$$

4. Farmer-Covert model K_3 same as Rayleigh except:

$$v' = \frac{\frac{k_m}{k_{3f}} + 1 + \frac{k_m}{ah_c}}{\frac{k_m}{k_{3f}} - 1 + \frac{k_m}{ah_c}} \quad (5.7)$$

where “a” is the fiber radius and h_c is the interface conductance.

Note that in Farmer-Covert model it's assumed that there is a thin interphase between the fiber and the matrix with known conductance. Farmer-Covert model reduces to the Rayleigh model if the conductance becomes very large.

5. Halpin -Tsai model is given by:

$$k_3 = k_m \left[\frac{1 + \xi \eta V_f}{1 - \eta V_f} \right] \quad (5.8)$$

where

$$\eta = \frac{\frac{k_{3f}}{k_m} - 1}{\frac{k_f}{k_m} + \xi}$$

when $\xi = 1$ Equation 1.7 can be written as:

$$k_3 = k_m \frac{V_f}{\frac{1}{k_f - k_m} + \frac{1 - V_f}{2k_m}}$$

Table 5.2 lists the calculated values of AS4/Graphite /Epoxy from the constituent properties listed in Table 5.1. The measured transverse conductivity (k_3) is 0.71 W/mk.

Table 5.2

Comparison between models.

Model	Calculated Conductivity, k_3 , W/mK
	AS4 Graphite fiber/epoxy
Chawla	0.657
Springer-Tsai	0.655
Rayleigh	0.710
Halpin-Tsai	0.669

5.6 Prediction of the Transverse Conductivity (k_3) for AS4/3501-6 Composite

Calculated transverse conductivity by prediction models also agrees with the experimental values measured as shown in Table 5.3.

Table 5.3

Comparison between predicted transverse conductivity (k_3) and experimental results

Model	Transverse Conductivity of AS4/3501-6 , W/mK
Chawla	0.82
Springer-Tsai	0.88
Rayleigh	0.94
Halpin-Tsai	0.83
Experimental result ($V_f= 0.67$)	0.69

5.7 Summary

Micromechanics models were used to calculate axial (k_1) and transverse (k_3) conductivities of AS43501-6 Carbon/Epoxy composites. The rule mixture was used to calculate the axial thermal conductivity (Equation 5.1). Constituent properties in Table 5.1 were used to

calculate the transverse conductivity as shown in Table 5.3. The result agrees with the experimental value, which is 0.69 W/mk.

CHAPTER 6

Concluding Remarks and Future Work

6.1 Concluding Remarks

Axial and transverse thermal conductivities of AS4/3501-6 unidirectional composite laminate were determined at temperature range from 20°C to 100°C. Differential scanning calorimeter was used to measure the specific heat capacity of the materials as per ASTM E-1269. The thermal diffusivity was measured using the flash method. Then the thermal conductivity was calculated from the product thermal diffusivity, specific heat capacity, and the density for a given temperature. The fiber reinforced composite properties are defined with respect to the orientation of the fibers in the lamina. There are three principal directions of the lamina (x_1 , x_2 , and x_3). The x_1 represents the fiber direction; x_2 and x_3 are perpendicular to the fiber directions. Properties in x_2 and x_3 are same because the unidirectional laminate transversely isotropic. Therefore the determination of the conductivity in x_1 and x_3 directions are sufficient to get all three dimensional properties of the laminate. Five samples were tested in each case, and then the thermal conductivity was calculated by using the equation:

$$k = \rho \cdot C_p \cdot \alpha \quad (6.1)$$

where k is the thermal conductivity, ρ is the density, C_p is the specific heat capacity, and α is the thermal diffusivity of the material. The density and specific heat are scalar they do not change with direction, only the diffusivity changes with the fiber direction.

The room temperature (20°C) specific heat capacity was 0.898 J/g°C, and the axial and transverse thermal diffusivities were 3.9×10^{-2} cm²/s and 5.4×10^{-3} cm²/s, respectively. The density of the thick specimens (axial test) and thin specimens (transverse test) were 1.42 g/cm³ and 1.41 g/cm³, respectively. The axial and transverse conductivities were 4.9

W/mK and 0.69 W/mK respectively. While transverse conductivity for the same material from the literature was 0.61 W/mK, respectively. The transverse conductivity differed by 10 %, which is reasonable. The micromechanics model predicted 4.5 W/mK and 0.75 W/mK for axial and transverse conductivities, respectively. The present experimental and analytical results agree within 10%.

Expressions for axial and transverse conductivities for different temperature were:

Axial conductivity:

$$k_1 = 4.8 + 1.37 \times 10^{-2}T \quad (6.2)$$

Transverse conductivity:

$$k_3 = 0.672 + 1.95 \times 10^{-3}T \quad (6.3)$$

where T is temperature in Celsius. The R value of least square fit was more than 0.95.

6.2 Future Work

The following suggestions for future work are made:

1. In this research axial and transverse thermal conductivities of the lamina were studied. For future work, thermal properties of multidirectional laminates can be explored and compared with macromechanics analysis.
2. Anter Flash equipment can be modified and improved to apply for cryogenic temperatures.
3. Continued thermal characterization of different composites is needed to develop a material database

References

1. Daniel, I.M. and O. Ishai, Engineering mechanics of composite materials. New York : Oxford University Press, 1994.
2. Cernuschi, F., et al., Thermal Diffusivity Measurements by Photothermal and Thermographic Techniques. p. International Journal of Thermophysics 25, no. 2 (2004): 439-457.
3. Cernuschi, F., et al., Comparison of thermal diffusivity measurement techniques. Quantitative InfraRed Thermography Journal, 2002.
4. Dasgupta, A. and R.K. Agarwal, Orthotropic Thermal Conductivity of Plain-Weave Fabric Composites Using a Homogenization Technique. p. Journal of Composite Materials v26 n18 (12/1992): 2736-2758.
5. Hexcel Corporation. (2013). HexTow® AS4 Carbon Fiber. Product Data. Retrieved from <http://www.hexcel.com/resources/datasheets/carbon-fiber-data-sheets/as4.pdf>
6. Sweeting, R. and X. Liu, Measurement of thermal conductivity for fibre-reinforced composites. Composites Part A: applied science and manufacturing, 2004. 35(7): p. 933-938.
7. Wetherhold, R.C. and J. Wang, Difficulties in the theories for predicting transverse thermal conductivity of continuous fiber composites. Journal of composite materials, 1994. 28(15): p. 1491-1498.
8. Saad, M. and B. Doleman, Thermal Characterization of AS4/3501-6 Carbon /Epoxy Composite. Frontiers in Heat and Mass Transfer (FHMT), 2013.

9. Balandin, A.A., Thermal properties of graphene and nanostructured carbon materials. *Nature materials*, 2011. 10(8): p. 569-581.
10. Klancnik, G., J. Medved, and P. Mrvar, Differential thermal analysis (DTA) and differential scanning calorimetry (DSC) as a method of material investigation, 2010. 57(1): p. 127-142.
11. TA Instruments. Thermal Analysis & Rheology, Sapphire Specific Heat Capacity Literature Values.
12. ASTM Standard E-1269. Standard Test Method for Determining Specific Heat Capacity by Differential Scanning Calorimetry. West Conshohocken, PA: ASTM International, 2005.
13. ASTM Standard E-1461. Standard Test Method for Thermal Diffusivity by the Flash Method. West Conshohocken, PA: ASTM International, 2007.
14. TA Instruments for measuring thermal diffusivity, thermal expansion and specific heat capacity., Anter Corporation.
15. Parker, W., et al., Flash method of determining thermal diffusivity, heat capacity, and thermal conductivity. *Journal of applied physics*, 1961. 32(9): p. 1679-1684.
16. Clark III, L. and R. Taylor, Radiation loss in the flash method for thermal diffusivity. *Journal of Applied Physics*, 1975. 46(2): p. 714-719.
17. Patrick, M.J., Examination of Thermal Properties of Carbon-Carbon and Graphitized Carbon-Carbon Composites, 2013.
18. Web.HexPly@3501Epoxy-Matrix; Available:
from: http://www.hexcel.com/Resources/DataSheets/Prepreg-Data-Sheets/3501_us.pdf.
19. NETZSCH. Operating Instructions DSC 200 F3 Maia Selb, Germany 2008.

20. Saad, M., D. Baker, and R. Reaves. Thermal Characterization of Carbon-Carbon Composites. in ASME 2011 International Mechanical Engineering Congress and Exposition. 2011. American Society of Mechanical Engineers.
21. Anter FlashLine™ Thermal Diffusivity Measuring System Operation and Maintenance Manual Part 1 Flashline 2000.
22. Hull, D. and T. Clyne, An introduction to composite materials. 1996: Cambridge university press.
23. Johnston, A.A., An integrated model of the development of process-induced deformation in autoclave processing of composite structures, 1997, University of British Columbia.
24. Tian, T., Anisotropic thermal property measurement of carbon-fiber/epoxy composite materials. 2011.